Energies **2010**, *3*, 1014-1048; doi:10.3390/en30501014

OPEN ACCESS

energies

ISSN 1996-1073

www.mdpi.com/journal/energies

Review

Exploiting Laboratory and Heliophysics Plasma Synergies

Jill Dahlburg [1,*], William Amatucci [1], Michael Brown [2], Vincent Chan [3], James Chen [1], Christopher Cothran [4], Damien Chua [1], Russell Dahlburg [1], George Doschek [1], Jan Egedal [5], Cary Forest [6], Russell Howard [1], Joseph Huba [1], Yuan-Kuen Ko [1], Jonathan Krall [1], J. Martin Laming [1], Robert Lin [7], Mark Linton [1], Vyacheslav Lukin [1], Ronald Murphy [1], Cara Rakowski [1], Dennis Socker [1], Allan Tylka [1], Angelos Vourlidas [1], Harry Warren [1] and Brian Wood [1]

1 Naval Research Laboratory, Washington, DC 20375, USA
2 Swarthmore College, Swarthmore, PA 19081, USA
3 General Atomics, San Diego, CA 92186, USA
4 Global Defense Technology and Systems, Inc., Crofton, MD 21114, USA
5 Massachusetts Institute of Technology, Cambridge, MA 02139, USA
6 University of Wisconsin, Madison, WI 53706, USA
7 University of California, Berkeley, CA 94720, USA

* Author to whom correspondence should be addressed; E-Mail: Jill.Dahlburg@NRL.NAVY.MIL; Tel.: 001-202-767-6343; Fax: 001-202-767-1116.

Received: 1 March 2010; in revised form: 5 May 2010 / Accepted: 18 May 2010 / Published: 25 May 2010

Abstract: Recent advances in space-based heliospheric observations, laboratory experimentation, and plasma simulation codes are creating an exciting new cross-disciplinary opportunity for understanding fast energy release and transport mechanisms in heliophysics and laboratory plasma dynamics, which had not been previously accessible. This article provides an overview of some new observational, experimental, and computational assets, and discusses current and near-term activities towards exploitation of synergies involving those assets. This overview does not claim to be comprehensive, but instead covers mainly activities closely associated with the authors' interests and reearch. Heliospheric observations reviewed include the Sun Earth Connection Coronal and Heliospheric Investigation (SECCHI) on the National Aeronautics and Space Administration (NASA) Solar Terrestrial Relations Observatory (STEREO) mission, the first instrument to provide remote sensing imagery observations with spatial continuity extending from the Sun to the Earth, and the Extreme-ultraviolet Imaging Spectrometer (EIS) on the Japanese *Hinode* spacecraft that is measuring spectroscopically

physical parameters of the solar atmosphere towards obtaining plasma temperatures, densities, and mass motions. The Solar Dynamics Observatory (SDO) and the upcoming Solar Orbiter with the Heliospheric Imager (SoloHI) on-board will also be discussed. Laboratory plasma experiments surveyed include the line-tied magnetic reconnection experiments at University of Wisconsin (relevant to coronal heating magnetic flux tube observations and simulations), and a dynamo facility under construction there; the Space Plasma Simulation Chamber at the Naval Research Laboratory that currently produces plasmas scalable to ionospheric and magnetospheric conditions and in the future also will be suited to study the physics of the solar corona; the Versatile Toroidal Facility at the Massachusetts Institute of Technology that provides direct experimental observation of reconnection dynamics; and the Swarthmore Spheromak Experiment, which provides well-diagnosed data on three-dimensional (3D) null-point magnetic reconnection that is also applicable to solar active regions embedded in pre-existing coronal fields. New computer capabilities highlighted include: HYPERION, a fully compressible 3D magnetohydrodynamics (MHD) code with radiation transport and thermal conduction; ORBIT-RF, a 4D Monte-Carlo code for the study of wave interactions with fast ions embedded in background MHD plasmas; the 3D implicit multi-fluid MHD spectral element code, HiFi; and, the 3D Hall MHD code VooDoo. Research synergies for these new tools are primarily in the areas of magnetic reconnection, plasma charged particle acceleration, plasma wave propagation and turbulence in a diverging magnetic field, plasma atomic processes, and magnetic dynamo behavior.

Keywords: heliophysics; laboratory plasma experiments; magnetohydrodynamics; plasma simulation

1. Introduction

We have arrived at a nexus in our ability to understand energy transport and release processes in a wide range of plasmas that are significant to modern society. For heliospheric plasmas, we are now able to observe and parameterize a vast wealth of Sun-driven plasma dynamics at many scales, hyperspectrally, and around the clock, and through many different levels of solar activity, from sunspot maximum to the recent extremely quiet solar minimum. These dynamical phenomena include, for example, solar flares and coronal mass ejections (CMEs) [1], solar active region plasma outflows [2], and solar bright points that produce plasma waves and jets [3]. Average physical properties of the Sun's upper atmosphere have also been revealed with compelling clarity [4]. The growing databases of well-documented observations are paving the way towards routine and accurate quantification of heliophysics plasma activity, the 'smoking-gun' sources of space weather at Earth, and thus towards reliable extended operational environments forecasting that is progressively necessary for full utilization of our many space-based technologies [5]. For confined laboratory plasmas, we are now able to explain with a remarkable degree of precision (e.g., Lukin *et al.* [6]) a broad range of reproducible confined fusion and basic plasma dynamics experiments. This skill hallmarks a deep

fusion energy sciences capability that is essential for the world's next step on the quest for the benign, clean, and limitless energy of fusion power on Earth: accurate understanding of the burning plasma confined fusion experiment, ITER [7].

Recent trends indicate that the modeling of the smoking-gun heliophysics activity for space weather at Earth is in need of a thoughtful, rigorous, and possibly laboratory-driven, methodology for verification and validation of simulation codes, to be able to meet the grand challenge of forecasting space weather. Further, although fusion plasma research has to date been outstandingly successful at evaluating plasma dynamics regimes that are accessible from the current suites of laboratory experimental devices, broader reaches of plasma dynamics configurations would provide beneficial new opportunities to test and enhance the robustness of current laboratory-based experimental diagnostics and predictive modeling tools, towards assaying the expected new parameter regimes [8] of ITER. The combination of the unique heliophysics databases that are growing at unprecedented rates from the active and powerful observatories such as the Solar Terrestrial Relations Observatory (STEREO) [9] and *Hinode* [10], and to be increasing with the Solar Dynamics Observatory (SDO) [11], the Interface Region Imaging Spectrograph (IRIS) [12] and Solar Orbiter [13], and well-understood plasma dynamics experimental environments that are currently available with vibrant ongoing and planned laboratory experiments [8,14], presents a rare and important opportunity for synergistic research in plasma physics that will advance both the heliospheric and the laboratory plasma physics areas of endeavor enormously.

The authors of this paper are involved in various aspects of solar and laboratory plasma research, some of which is noted above. This paper is the result of a small gathering attended by the authors in February 2009 in the Space Science Division at the U.S. Naval Research Laboratory (NRL) with the goal of defining methods for combining their solar, theoretical, and laboratory research to exploit the obvious synergies of their research. This article is therefore not a comprehensive review of all of the on-going work linking laboratory and astrophysical plasmas, which is currently quite extensive. However, it does consider new state-of-the-art observations of the Sun, new state-of-the-art numerical simulation codes, and some sophisticated laboratory plasma experiments that might be combined to increase greatly our understanding of the physics of plasmas.

The potential synergies of our research are quantitatively rooted in the shared parameter space of heliospheric and laboratory areas of plasma physics research. This is illustrated by the good overlap and shared parameter ranges of our interests as evidenced in Figure 1, a plot of the electron density (n_e) and temperature (T_e) ranges of operation for a characteristic set of current confined plasma experimental devices, and the n_e, T_e parameter ranges of representative heliospheric phenomena.

As may be inferred from Figure 1, the plasma research investigations of heliospheric and laboratory plasmas share fundamental aims. The US National Aeronautics and Space Administration (NASA) heliophysics roadmap [15] defines four basic research focus areas towards the major programmatic goal of space environmental prediction: understanding the multi-scale process of magnetic reconnection; understanding the plasma processes that accelerate and transport particles; understanding the ion-neutral interactions that couple neutral and ionized species; and, understanding the creation and variability of magnetic dynamos and the generation of magnetic fields in widely different environments. The US Department of Energy (DOE) Office of Science (SC) "Scientific Challenges, Opportunities and Priorities of the US Fusion Energy Sciences Program" [16] define nearly identical

key basic research campaign areas, under that program's overarching themes of understanding matter in the high temperature plasma state, and creating a star on Earth. The fusion energy sciences research planning campaigns include: macroscopic plasma physics, to understand the roles of magnetic structure on plasmas; multi-scale transport physics, to understand the physical processes that govern magnetic reconnection and energy dissipation, generate electromagnetic fields and possibly turbulent flows, and control the confinement of heat, momentum, and particles in plasmas; and, waves and energetic particles, towards understanding how electromagnetic waves and high-energy particles interact with and control high-temperature plasmas. The central planning document of each of the heliophysics and the laboratory plasma scientific communities hence positively supports the synergistic new research that is described herein.

Figure 1. The electron density and temperature operating regimes of an illustrative group of current laboratory confined plasma experiments, plotted together with the observed parameter space that is accessed by elemental heliospheric phenomena.

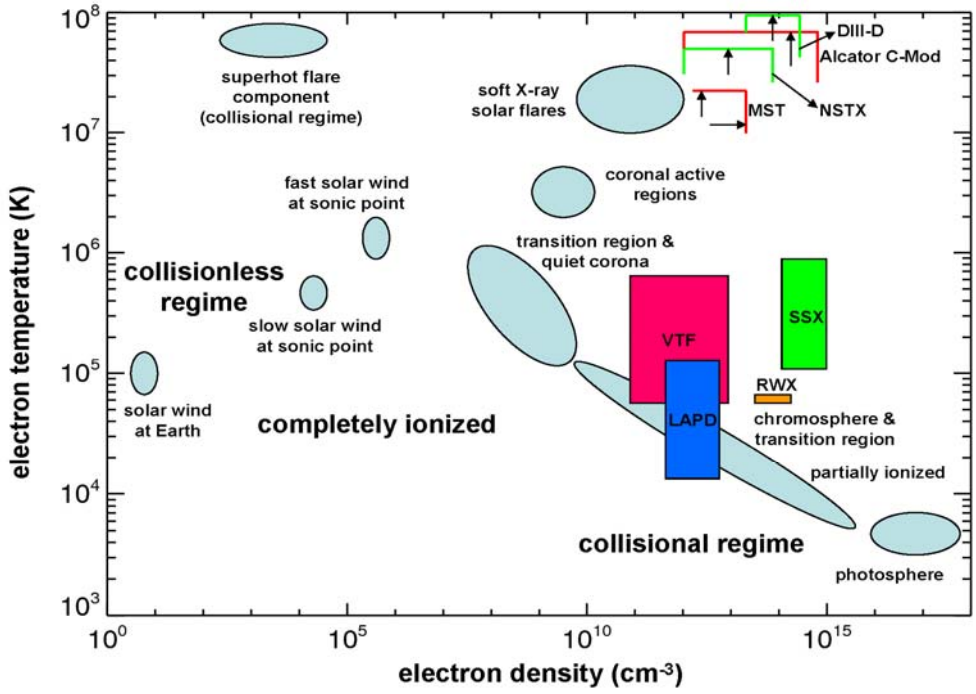

Following a discussion of fundamental plasma physics areas that are ripe for coupled heliophysics and laboratory plasmas collaborative research, this paper delineates an illustrative but far from exhaustive subset of the heliophysics, laboratory experimental, and developing modeling capabilities that are now available for application to these investigations. We conclude with a summary of the experimental areas that we identify as most promising and provide an outline for next steps.

2. Identified Areas for Possible Coupled Research

Historically, the real basis for advance in the physical sciences has been by means of laboratory experimentation [17]. While heliophysical and laboratory plasmas are of vastly different scales both temporally and spatially, much of the essential dynamics exhibits scale-similarity. Further, laboratory

research enables reproducible investigation of key small-scale processes that can be of central significance. Examples of successes that span across laboratory and heliophysical plasma physics research include the development of accurate atomic physics databases [4]; shuttle reentry and aeronautical flight [18]; and, understanding whistler wave dynamics [19–22]. The NRL gathering participants, all of whom are co-authors of this report, identified the following areas that are ready for coupled research in space-based Sun-Earth system research and laboratory-based confined plasma research. Data gathered from both environments in these areas will serve to validate and advance theoretical and numerical models and tools.

2.1. Magnetic Reconnection

Magnetic reconnection in both confined laboratory and open heliophysical plasmas is believed to be the dominant agent of dynamical activity and energy conversion, such as the sawtooth instability and major disruptions in toroidal confined systems, and flares and CMEs in the solar corona. However, the physical mechanisms that initiate reconnection remain elusive because of the broad ranges of geometries and length scales involved. For instance, solar reconnection occurs at scales of 10's of meters, well below those which are currently observable. With the caveat that laboratory plasmas and solar plasmas might be irreconcilably different for reasons that include skin depths (which are much shorter relative to plasma dimensions in the solar corona than in laboratory plasmas), and magnetic field line configurations (which are open in the corona and for the most part closed in existing laboratory facilities): a more complete understanding of magnetic reconnection can be found by concerted simultaneous study of this phenomenon across both laboratory and solar regimes.

One configuration that provides an appropriate test bed for synergistic investigation is that of the magnetic flux tube or loop (e.g., Linton [23], and references therein). A solar flare loop is bright because it confines heated, relatively dense plasma, and the flux-tube magnetic field provides a conduit, *i.e.,* it is a 'plasma-guide'. Active region and flare coronal loop magnetic fields are line tied in the Sun's photosphere/chromosphere at both ends, e.g., Krall and Chen [24]. Currently it is believed that solar flares are energized by magnetic reconnection in the corona that simultaneously changes the magnetic field topology to create flare loops and releases magnetic energy into those loops as kinetic and thermal energy. This released magnetic energy drives beams of particles and thermal conduction fronts down to the bases of the loops, where they impact the chromosphere and drive ablated X-ray emitting multi-million degree plasma back up into the closed coronal loops. Flares frequently consist of a large number of such loops in an arcade, indicating multiple reconnection sites (Figure 2).

For understanding solar magnetic reconnection-based processes such as solar flare energy release and coronal heating in general, key questions include: To what extent is plasma confined in a loop? Is a loop truly a loop, or a manifestation of something different? and, How does magnetic reconnection occur in line-tied systems? While a growing body of theoretical literature indicates that reconnection and secondary instabilities are altered by the line-tying [26,27], there have not been many laboratory experiments devoted to this particular problem. It would be of great interest to develop such experiments, for example, twisting line-tied plasmas to investigate the spontaneous development of current sheets (also termed solar sub-resolution strand models, or nanoflares). Can reconnection occur in open magnetic field configurations, and if so: what sort of trigger would most likely set off

reconnection in an open-field solar plasma? Once initiated, reconnection then propagates in both laboratory and solar plasmas, leading to the question: Is the propagation of spontaneous magnetic reconnection in a loop or along a solar flare arcade a physically similar process to the propagation of spontaneous reconnection around the Massachusetts Institute of Technology (MIT) Versatile Toroidal Facility (VTF) laboratory torus (Figure 3 [28]; and, Section 4.4 following)? Could laboratory experiments on unstable loops be extended to investigate CME evolution? Finally, it is not known if a loop contains axial current, which is related to how the photosphere may affect solar coronal dynamics, and it would be of value to address the effects and signatures of an axial magnetic current in a laboratory line-tied configuration.

Figure 2. Left: TRACE image (171 Å) of magnetic loops. Right: *Yohkoh* image of soft X-ray loop and hard X-ray footpoint and loop top emission [25].

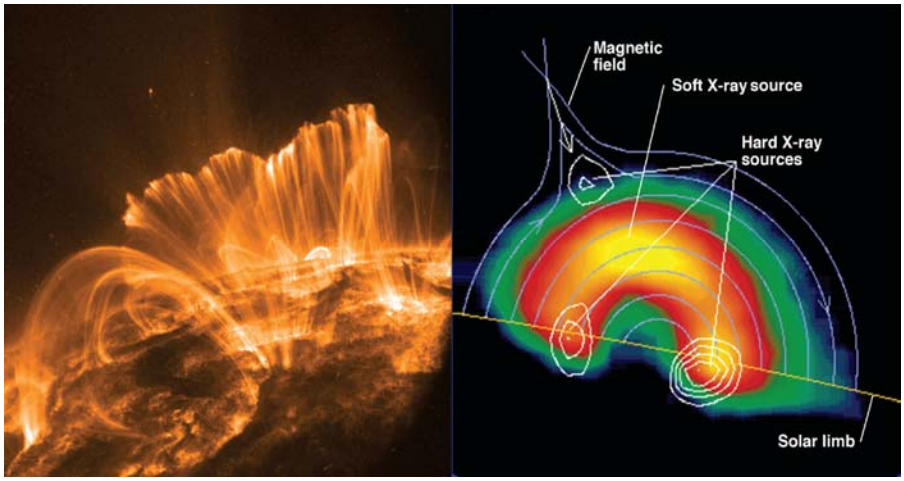

Figure 3. A laboratory spontaneous magnetic reconnection event in the Massachusetts Institute of Technology VTF [28], depicted by measured contours of the plasma density, floating potential, current density, and the reconnection rate. The overlaid lines represent contours that coincide with the potential projection of magnetic field lines; see also Section 4.4, following.

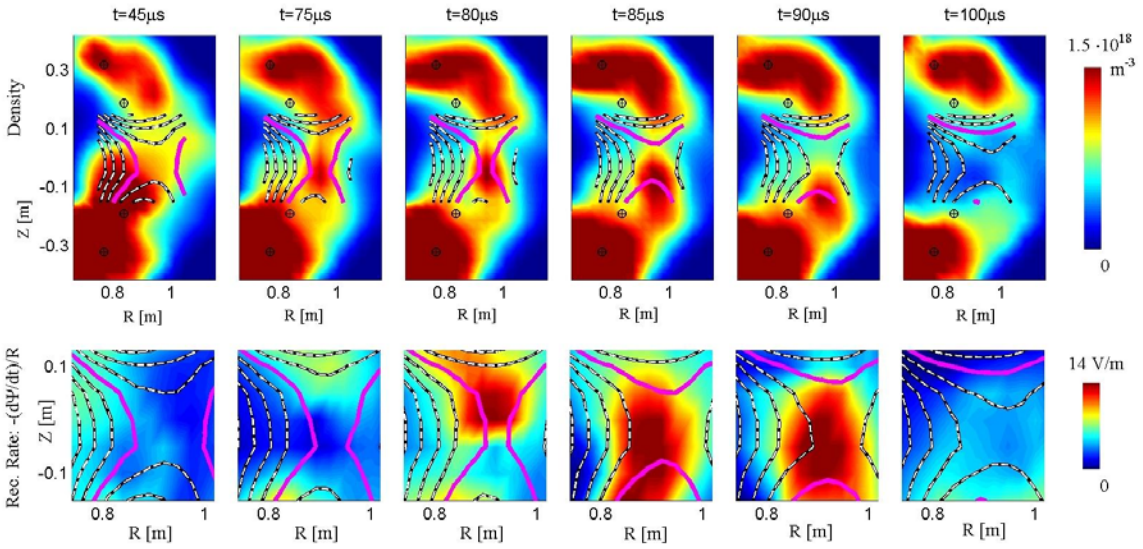

2.2. Plasma Charged Particle Acceleration

Understanding plasma charged particle acceleration contributes to advances in confined plasma heating, particle accelerators, and elucidation of solar plasma constituent distributions and solar abundances. Solar physics observation of particle acceleration and energy release is outstandingly exemplified, for instance, by the *RHESSI* (Reuven Ramaty High Energy Solar Spectroscopic Imager) imaging and spectroscopy observations of the 23 July 2002 gamma-ray line flare that is reported by Lin *et al.* [29].

Figure 4. Left: An X-10 flare on 29 October 2003. The green image is a TRACE 195 Å filter image [29] that shows the flare arcade loops at high spatial resolution. Two *RHESSI* energy channels are also shown. The lower energy channel corresponds to the loop tops near the reconnection region while the higher energy is probably thick target Bremsstrahlung from the footpoints. Right: An X-ray/gamma-ray spectrum from a gamma-ray flare.

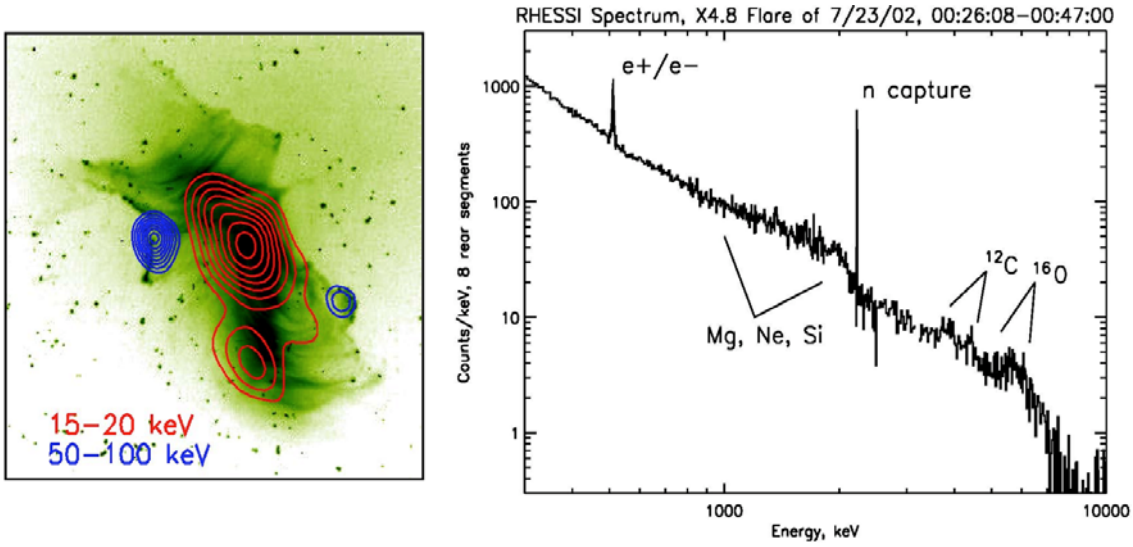

An organizing question for coupled research in this area is: Can the mechanisms causing solar abundance variations be investigated in the laboratory? Preferential heating of heavy ions is suspected in the solar atmosphere, and two fundamentally different abundances are found in fast and slow solar wind streams in *in situ* measurements. Solar abundances are observed to vary by a factor of 3–4 according to the first ionization potential (FIP) effect (Figure 5). Emerging active regions have photospheric abundances but these get converted over time to coronal abundances (enhanced low-FIP (< 10 eV) abundances compared to photospheric abundances). In the solar corona, closed loop regions have coronal abundances while open field regions that are sources of the fast solar wind have close to photospheric abundances. Abundance variations might be used to locate the origin of the slow solar wind. These variations are currently believed to be the result of the ponderomotive force in the chromosphere, which preferentially lifts chromospheric ions-but not neutrals-into the corona. The Alfvén waves giving rise to this ponderomotive force may have a coronal or photospheric origin, with the coronal origin appearing more likely in the solar case at the present time (see Figure 5 [30]).

An abundance enhancement experiment in the laboratory, to investigate the evolution of relative abundances in a hot plasma, would be very interesting. Such an experiment would address the question: Could contracting magnetic islands, which may accelerate electrons, also explain mass bias injection efficiency, and could this be examined in the laboratory? The idea would be to construct an experiment that would test whether the 'old ion acceleration mechanism'-sawtooth along the toroidal magnetic field - or the 'new ion acceleration mechanism'-heating from island bounce-is more effective. This would also be an important laboratory experiment for investigating particle acceleration in flares, where multiple islands due to reconnection might occur. A related question is: How does the electron non-thermal distribution evolve for the two different acceleration mechanisms? Another important issue would be to understand the turbulence generated by such events, which would generate the FIP effect in propagation away from the reconnection site and reflection at the chromospheric loop footpoints.

Figure 5. Schematic illustrating the First Ionization Potential (FIP) effect model of Laming (2009) [30]. Alfvén waves are incident on the coronal loop from below on the right hand side. Waves are either transmitted into the loop or reflected back down again. Waves in the coronal loop bounce back and forth, with some leakage at each footpoint, giving rise to a ponderomotive force in the steep density gradients of the chromosphere. This force preferentially accelerates chromospheric ions into the coronal thereby enhancing the coronal abundance of low FIP ions [31].

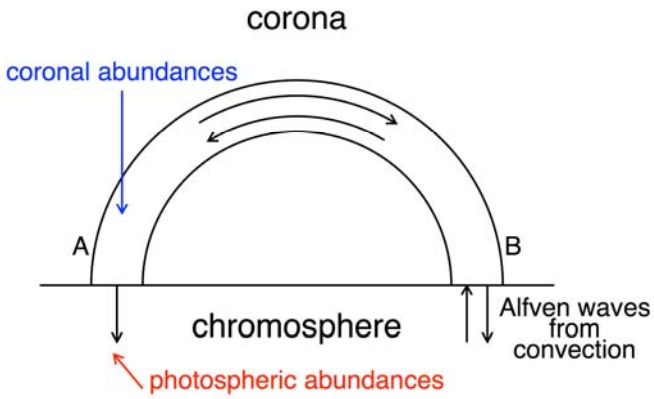

2.3. Plasma Wave Propagation and Turbulence in a Diverging Magnetic Field

The propagation and interaction of electromagnetic and electrostatic waves in plasmas is much studied and generally quantitatively well-understood. A key area of open research remaining is that of the dynamics of wave propagation and turbulence in the presence of diverging magnetic fields such as the solar wind.

Charge states in the solar wind are higher than those expected in the source region on the Sun; $Fe^{+9\text{-}+11}$ are commonly abundant in the fast solar wind as measured at the Lagrange L1 point by the Advanced Composition Explorer (ACE), while Fe^{+8} ions are expected to dominate in coronal holes that are the sources of the fast solar wind. This implies that the solar wind is heated as it is accelerated. Density and velocity shear could heat the solar wind electrons [31,32]. Imaging observations during eclipses support this view [33]. The acceleration of the solar wind itself is usually taken to be due to

ion cyclotron wave heating of ions, increasing their velocities perpendicular to the magnetic field, which are then converted to parallel velocity under the action of the adiabatic invariant in diverging field lines. However, where do ion cyclotron waves come from in the solar wind? (How are ion cyclotron waves excited and under what conditions in the solar wind?) This is an open question. For instance, waves generated from the surface should be absorbed completely by heavy ion cyclotron resonance, in which case light ions such as oxygen ions would not be accelerated, contrary to observations. There are processes in laboratory plasmas that could shed light on this difficulty, which possibly could be simulated by charge (gyro?)-kinetic turbulence codes that model bump-on-tail distributions. A laboratory experiment that measures the velocity of plasma flow in a diverging magnetic field could address the question: Do ions propagating in a diverging magnetic field get accelerated (as a result of ion cyclotron wave absorption)? What are related electron non-thermal distribution effects?

Laboratory plasma turbulence experiments in a diverging magnetic field could address key aspects of the propagation of structures in the solar wind. Kataoka *et al.* [34], for instance, report the numerical use of a spheromak-type magnetic field to model CME propagation in the solar wind, and find that many observed macro-structures are reproduced. For the slow solar wind, one could vary the laboratory experimental plasma density by a factor of two (since density and electric field are closely tied and convective cells are caused by electric fields), and look at convection of density macro-structures, to provide an important benchmark for ongoing major questions that are very relevant to predictive models of the heliosphere: How do density fluctuations evolve in a diverging magnetic field? Are they primarily passively advected, or is macroscopic turbulence generated? For the fast solar wind, a promising configuration to investigate the formation and acceleration would be the evolution of a three-dimensional, gravitationally stratified magnetofluid with line-tied magnetic fields subject to convection by fluid motions at the base of the system, and with outflow at the top. For the fast wind, electron microturbulence generated by ion cyclotron conditions also could be investigated. These experiments possibly could be performed in an existing device such as the NRL Space Physics Simulation Chamber [19–22] (see Section 4.3 following), or in other large linear devices such as LAPD [35] at the University of California, Los Angeles.

2.4. Plasma Atomic Processes

The primary source of information about the solar atmosphere, especially close to the Sun, is obtained via X-ray through ultra-violet (UV) spectroscopy, and the application of plasma diagnostics to the interpretation of the spectra. Close to the Sun where the solar plasma may be considered thermal, *i.e.,* a Maxwellian distribution of electrons, spectral line excitation is produced primarily by collisions with electrons. In the steady-state regime, electron impact ionization is balanced by radiative recombination and dielectronic recombination, and solar abundant ions appear with maximum fractional abundance in different temperature regions of the solar atmosphere, depending on the element and charge. This is in contrast to certain other astrophysical regimes where ionization balance is produced by photoionization followed by recombination (e.g., the star RR Tel [36]), or outflows associated with accreting objects [37]. Under solar conditions, spectral line intensity ratios can be used to determine electron temperatures and densities, and relative element abundances. Absolute

abundances can be determined from line to continuum ratios. In certain cases, departures from ionization equilibrium and non-Maxwellian electron distributions can also be inferred from line ratios. Furthermore, above the chromosphere (where $T_e > 20 \times 10^4$ K) spectral lines are primarily optically thin and radiative transfer effects can usually be ignored. The spectral line profiles can be used to infer ion temperatures and/or non-thermal mass motions, and bulk plasma motions along the line-of-sight. In the case of the O^{+5} ion, both collisionally and radiatively excited, even more information can be extracted from the line intensities and profiles due to the phenomenon of Doppler dimming (e.g., Withbroe *et al.* [38]). In addition to plasma diagnostics of small-scale features in the atmosphere, it is highly desirable to measure or construct proxies for the total solar X-ray, extreme UV (EUV), and UV irradiance (the Sun-as-a-star spectrum) for practical applications regarding the Earth's climate and global warming.

In solar spectroscopy, it is necessary to know where in the complex morphology of the Sun's atmosphere the spectral lines are emitted. Otherwise, the spectral information cannot be used effectively in understanding the physics of the atmosphere, such as what causes coronal heating, and how solar flare and coronal mass ejection energy is stored and released. Thus, the most desirable solar spectrometer is an instrument with high spectral and temporal resolution with the additional capability of constructing images either by rastering or the use of wide slits (slots). Such instruments are just now being designed, built and flown, *e.g.,* the Extreme-ultraviolet Imaging Spectrometer (EIS) on *Hinode* (see Figure 6) [10] and the *VERIS* sounding rocket payload under construction at NRL.

Applications of plasma diagnostics of highly ionized atoms to solar plasmas require accurate atomic data for ionization and recombination coefficients, electron (and sometimes proton) impact excitation rate coefficients, and radiative decay rates. For some ions many configurations and levels must be considered, and in most cases resonances in the excitation cross sections must be calculated in great detail. However, the plasma atomic physics modeling needed to diagnose solar plasmas relies almost entirely on theoretical calculations. There are some cases, *i.e.,* line ratios dependent only on atomic parameters, where solar data can be used to check calculations, but in the vast majority of cases the solar analyses are entirely dependent on theory. We have found that this theory is generally quite reliable, but in important situations considerable theoretical improvement is desired.

Figure 6. Left: Iron line spectrum of a solar flare recorded by X-ray spectrometers on the US Department of Defense (DoD) Space Test Program (STP) P78-1 spacecraft compared with a tokamak spectrum from the Princeton Large Torus. Right: The extreme-ultraviolet spectrum of solar quiet and active regions obtained by the EIS instrument on the *Hinode* spacecraft.

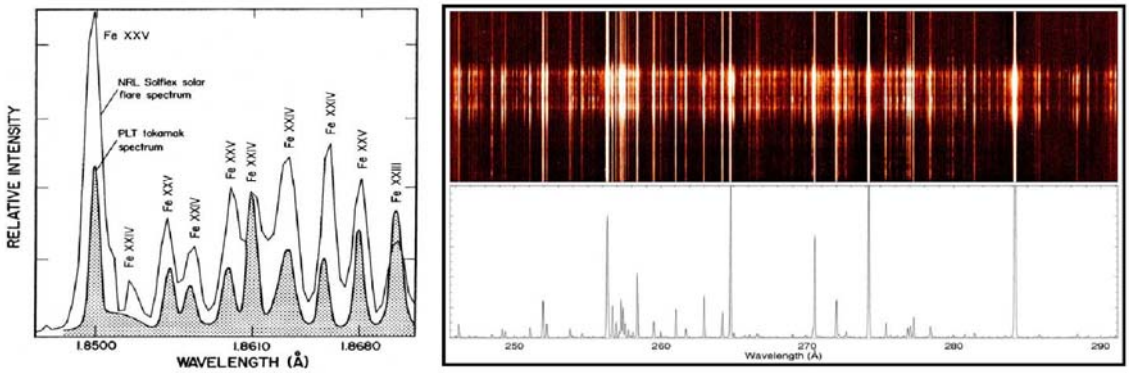

Tokamak plasmas can be similar to solar flare plasmas, but with somewhat higher electron densities. This difference does not in many cases produce fundamental differences between solar and tokamak plasma spectroscopy. In the past, the same type of spectroscopy used to diagnose solar plasmas has been used to diagnose some tokamak plasmas. However, tokamak and other laboratory confined plasma experiments also have additional methods for determining plasma parameters, and can be created where conditions such as temperatures and densities are well-known independent of spectroscopy. Obtaining X-ray and EUV spectra of such a plasma could provide a valuable check on the atomic physics used in solar plasma diagnostics. It should be possible to design a tokamak experiment that would, for example, obtain spectra within the EIS spectrometer range and then be applied to check the solar theory currently used in EIS analyses that depends on spectral lines from Fe VIII – Fe XVI. This would be a highly valuable laboratory plasma contribution.

In addition to tokamak plasmas, Electron Beam Ion Trap (EBIT) experiments have been used to measure electron impact excitation cross-sections for applications to solar plasmas [39–41]. Since the EBIT forms a mostly mono-energetic electron beam that is unidirectional, polarization diagnostic techniques can also be investigated with an EBIT machine.

Worthwhile plasma magnetic confinement laboratory experiments could be developed to advance diagnostics development and test atomic parameters, which would be of considerable interest for a range of future solar and laboratory spectroscopic experiments.

2.5. Magnetic Dynamo Behavior

The behavior of the solar magnetic dynamo determines the length of the solar cycle, and understanding the dynamos of the Sun and of the Earth is essential for describing the coupled Sun-Earth system. Hence, predictive understanding of dynamos and the generation of magnetic fields is recognized as a fundamental heliophysics area of research [15]. Currently, however, dynamo theories are extremely poor at making predictions [42], and there are many very basic questions about the solar dynamo, e.g., How does the dynamo depend on the Sun's rotation rate and the depth of the tachocline? and Are there tidal effects? It would be of profound interest and importance to develop a laboratory dynamo experiment that would drive magnetic dynamo activity and look at the dynamo problem 'inside out'. Such an experimental platform would also serve as a test bed for magnetohydrodynamic (MHD) codes modeling of inverse helicity cascades [43], the process that is thought to provide the underlying explanation for magnetic field generation throughout the universe.

3. Representative Heliophysics Observatories

NASA, the European Space Agency (ESA) and the Japanese Aerospace Exploration Agency (JAXA) have collaboratively developed a network of spacecraft that is often strategically termed the Heliophysics Great Observatory. A few key experiments from this body of satellites, data from which will outstandingly further the synergistic research described above, are highlighted in this Section.

3.1. STEREO / SECCHI

SECCHI, the Sun Earth Connection Coronal and Heliospheric Investigation [9], is a NRL-led suite of five scientific telescopes that are observing the solar corona and inner heliosphere from the surface of the Sun to the orbit of the Earth. These unique observations are being made in stereo by instrument suites on the NASA Solar Terrestrial Relations Observatory (STEREO) mission that launched in October 2006, with also SECCHI integration funding from the DoD STP. The twin STEREO spacecraft, STEREO-A and -B, were launched together and used a gravity assist from the Moon to place one of them in a prograde and the other in a retrograde heliocentric orbit, with each drifting away from the Earth at an average rate of about 22.5 degrees per year. Results from SECCHI are providing first-ever views of the heliosphere (Figure 7), and are fundamentally advancing our ability to forecast the arrival and effects of fast Earth-directed CMEs on the geomagnetic field and ionosphere [44].

Figure 7. SECCHI imagery captures a solar storm propagating through the heliosphere.

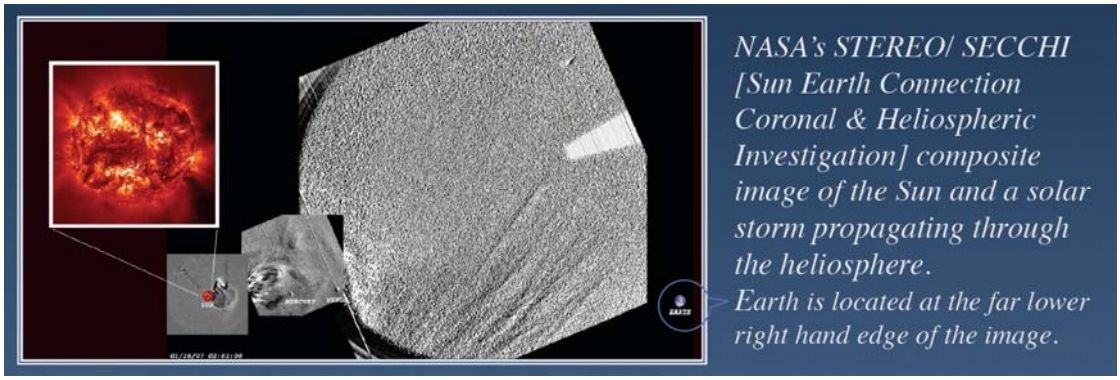

Figure 8. NRL-led space-based solar corona experiments (yellow diamonds).

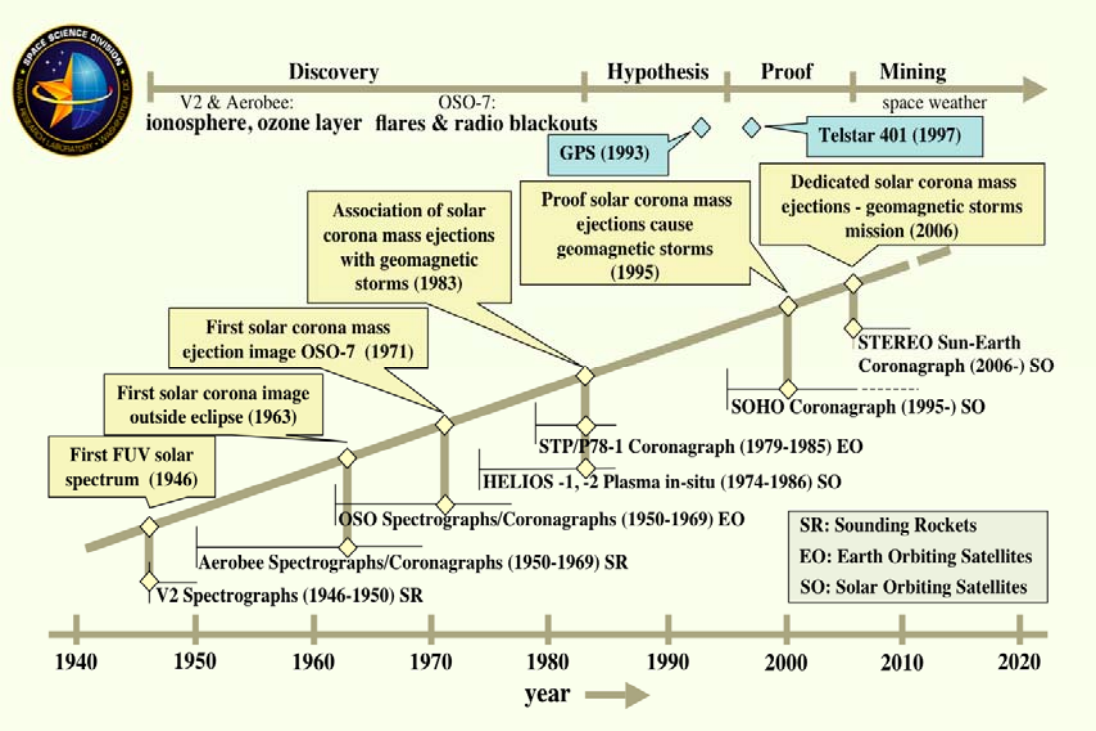

SECCHI is the newest in a series of space based imaging experiments of the solar corona that have been led by the NRL SSD, as illustrated by the timeline in Figure 8. Under the auspices of NASA, SECCHI heliospheric data are freely available to all researchers.

3.2. Hinode EIS

EIS (Figure 9) is the Extreme-ultraviolet Imaging Spectrometer [10] launched on the Japanese *Hinode* spacecraft in September 2006, along with a solar optical telescope (SOT) and a grazing incidence X-ray telescope (XRT). The state-of-the-art EIS spectrometer was built by an international collaboration, the leading institutions being the University College London-Mullard Space Science Laboratory (UCL-MSSL), the NRL SSD (through NASA), and the National Astronomical Observatory of Japan. UCL-MSSL leads the overall effort. EIS obtains high-resolution spectra in two EUV wavebands: 170–210 Å and 250–290 Å. The spatial resolution of EIS is 2" (1400 km on the surface of the Sun) and the spectral resolution is 0.0223 Å per pixel. EIS is fully meeting its science objective of measuring spectroscopically physical parameters of the solar atmosphere such as temperature, density, and dynamical properties over a temperature range from about 1×10^5 K to 20×10^6 K, at a spectral resolution sufficient to measure plasma flows of 2-3 km/s, and at a time cadence ranging from a few seconds to several minutes. The instrument heritage derives from the slitless NRL S082-A spectrograph aboard *Skylab*, and laser-produced plasma experiments in the NRL Plasma Physics Division (PPD).

Figure 9. An NRL space scientist aligns optics on the Extreme-ultraviolet Imaging Spectrometer (EIS) at Rutherford Appleton Laboratory (RAL) in the United Kingdom. EIS component testing was carried out at NRL and on the NRL SSD beamline facility at Brookhaven National Laboratory. End-to-end calibration was performed at RAL prior to shipment to Japan for integration onto the Solar-B (*Hinode)* spacecraft.

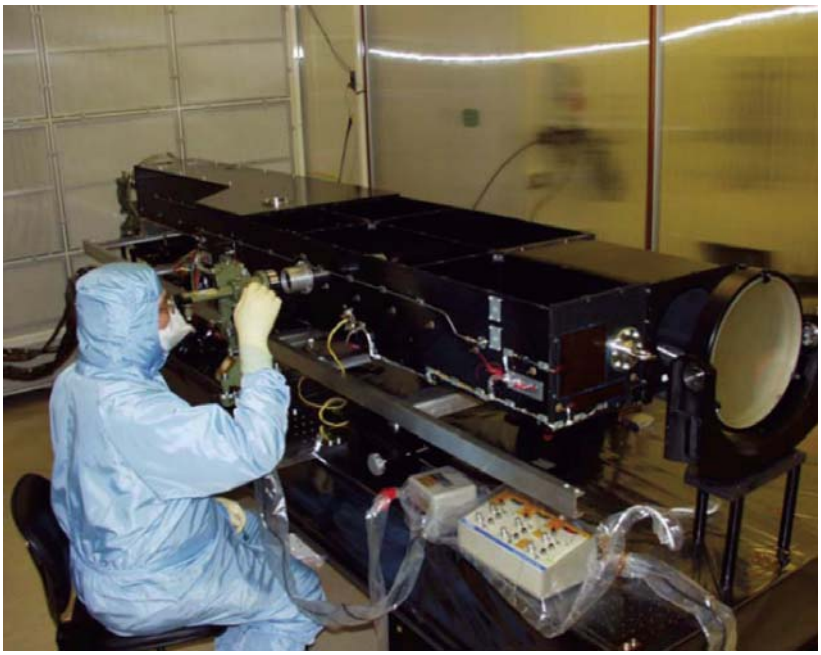

3.3. Solar Dynamics Observatory

NASA's Solar Dynamics Observatory (SDO) launched in February 2010 to explore the fundamental nature of solar magnetism and how it produces the solar cycle effects that influence Earth. SDO will provide high-cadence measurements of the interior of the Sun, the Sun's magnetic field, the hot plasma of the solar corona, and the irradiance that creates the ionosphere, towards understanding the solar variations that influence life on Earth [15]. The SDO mission science objectives are to improve understanding of these seven science questions [11]: What mechanisms drive the quasi-periodic 11-year cycle of solar activity? How is active region magnetic flux synthesized, concentrated, and dispersed across the solar surface? How does magnetic reconnection on small scales reorganize the large-scale field topology and current systems and how significant is it in heating the corona and accelerating the solar wind? Where do the observed variations in the Sun's EUV spectral irradiance arise, and how do they relate to the magnetic activity cycles? What magnetic field configurations lead to the CMEs, filament eruptions, and flares that produce energetic particles and radiation? Can the structure and dynamics of the solar wind near Earth be determined from the magnetic field configuration and atmospheric structure near the solar surface? When will activity occur, and is it possible to make accurate and reliable forecasts of space weather and climate?

3.4. Solar Orbiter SoloHI

When aloft on the ESA-NASA collaborative Solar Orbiter space mission, the NRL-led Solar Orbiter Heliospheric Imager (SoloHI) will continue and improve upon the very exciting observations of the inner heliosphere by the SECCHI suite aboard the STEREO mission. SoloHI (Figure 10) will double the field of view of SECCHI's Heliospheric Imager -1 (HI-1), and at greater resolution. SoloHI will image both the quasi-steady flow and transient disturbances in the solar wind, enabling detailed and timely contextual investigation of conditions that drive solar disturbances through the heliosphere and hence space weather at Earth.

Figure 10. SoloHI field-of-view (FOV) from the Sun (red circle to the right) through the heliosphere, as compared with SECCHI's Heliospheric Imagers HI-1 and HI-2.

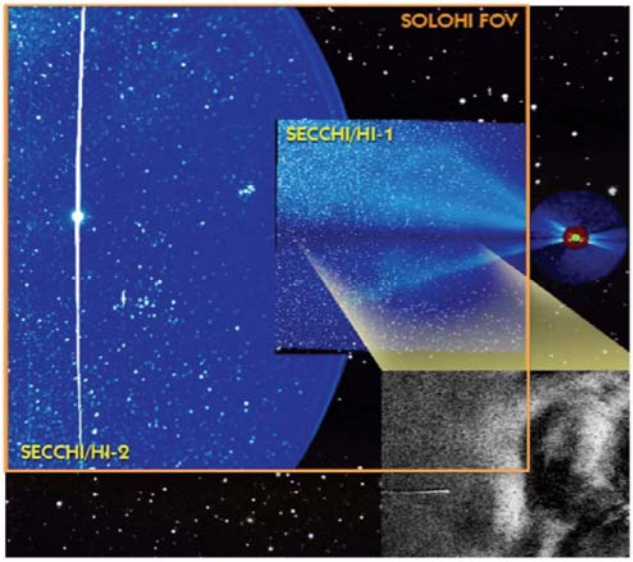

4. Illustrative Laboratory Confined Plasma Experiments

We here present an admittedly incomplete range of laboratory plasma experimental devices that offer compelling capabilities towards the synergistic research that is described in Section 2 above.

4.1. The Three Major US Toroidal Magnetic Fusion Facilities

The three major toroidal magnetic fusion facilities in the United States fusion energy sciences portfolio are C-Mod, DIII-D, and NSTX. Each of these facilities is world leading in fusion energy science research. We note these facilities here, for the reason that each also accesses plasma regimes and configurations of great interest for the investigations considered herein.

C-Mod (MIT) research is directed towards understanding plasma behavior at very high magnetic field with the plasma pressure and field appropriate for sustaining a burning plasma for energy production. C-Mod research contributes to the understanding of multiscale plasma transport and MHD behavior and stability [8].

DIII-D (General Atomics) is the US centerpiece capability in plasma transport, control of MHD instabilities, divertor physics, and development of the scientific basis for advanced tokamak operations. DIII-D research is directed towards understanding and improving plasma confinement and stability as a function of plasma shape and magnetic field distribution in a collisionless plasma. The DIII-D integrated multiscale plasma transport program performs measurements over the important wavelength ranges of the turbulent instabilities responsible for observed tokamak transport, and performs calculations with the most comprehensive gyrokinetic transport model in the world. Research also continues to be directed towards MHD plasma shaping, stability, and active instability control [8]. Also of interest are DIII-D post-shot 'afterglow' plasma conditions, which can closely approximate those of the extended solar corona.

NSTX (Princeton Plasma Physics Laboratory) performs research to apply advances in understanding of magnetic field configuration to optimize both plasma stability and confinement in a low-aspect-ratio toroidal experiment, or spherical torus. NSTX research is directed to exploring high-beta stability and confinement at extreme toroidicity, where beta is the ratio of plasma pressure to the magnetic field pressure. NSTX research is also directed towards investigation of multiscale plasma transport [8].

4.2. Line-Tied Magnetic Reconnection and Magnetic Dynamo Research at the University of Wisconsin

Insightful line-tied magnetic reconnection experiments have been performed at the University of Wisconsin at Madison (UW-Madison) with a linear screw pinch (Figure 11) constructed for studying the effects of different boundary conditions on ideal MHD activity [45]. When plasma production and lifetime are long compared to the growth of the MHD instabilities, this research is relevant to coronal heating magnetic flux tube observations and simulations. The screw-pinch experiment is 1.2 m long and has a plasma radius that can be varied from 3 to 10 cm. Four solenoidal magnets generate the steady-state axial field, adjustable to 1000 G. Nineteen electrostatic guns packed in a hexagonal array nominally produce a plasma with electron density n_e of ~4×10^{13} /cm^3 and temperature T_e of ~2 eV.

Figure 11. A schematic of the UW-Madison line-tied pinch experiment. The solenoidal magnets produce a nearly uniform magnetic field between the two ends. The anode plate is on the left and drawn to highlight its electrical conductivity. The hexagonally packed cathode array of plasma guns (shown on the right) breaks into three independently controllable regions of plasma represented by shadings in gray.

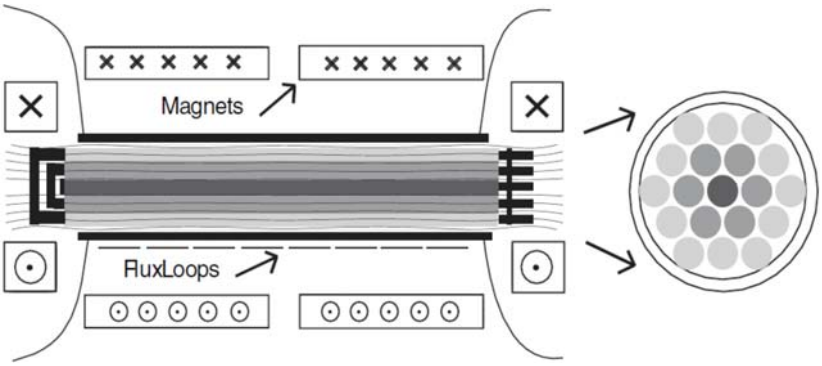

Figure 12. a. The Madison Plasma Dynamo Experiment (MPDX) under construction at the UW-Madison. b. The flux contours for the MPDX; the ring cusp magnetic field is generated by axisymmetric rows of 1.2 Tesla dipole magnets with alternating polarity. c. Alternating positive and negative electrostatic bias is applied to electrodes between cusp rings; the resulting torque from the plasma current crossed into the magnetic field causes the plasma to rotate about the symmetry axis and can be used for generating a variety of velocity fields.

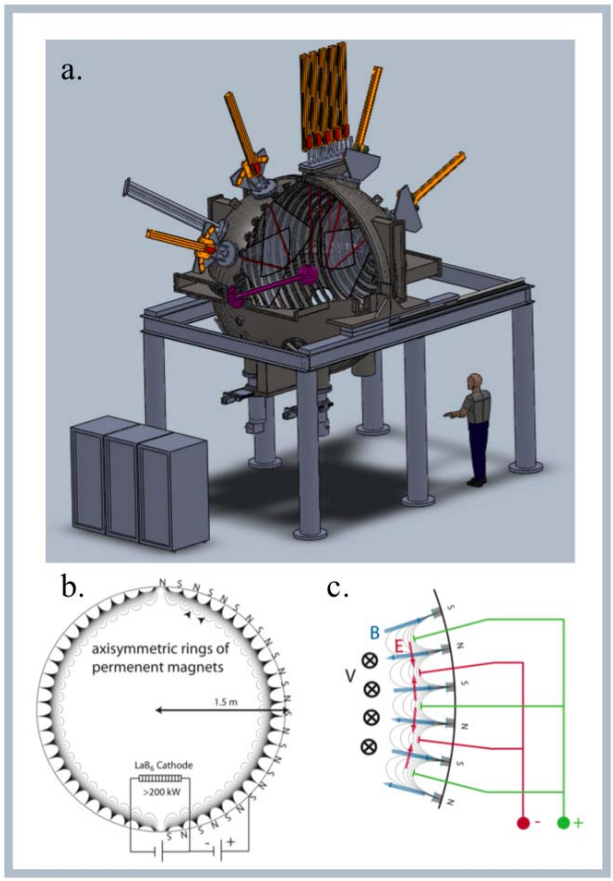

There is a clear scientific opportunity to operate a plasma physics dynamo experiment exploring very high beta plasma physics in which a fast flowing, hot plasma is confined in a largely magnetic field free volume, as depicted in Figure 12 [46]. This opportunity builds upon the excitement in recent years of using liquid metals to study dynamos, and will extend these studies to more astrophysically relevant parameters. Such a medium scale facility using plasmas, rather than liquid metals, is under construction at the UW-Madison (construction has been funded by the National Science Foundation) and could be used to study a host of questions related to magnetic field self-generation. Use of a plasma for this experiment will allow the magnetic Reynolds number (R_m), the dimensionless parameter governing self-excitation of magnetic fields, to be approximately a factor of 10 larger than in liquid metal experiments and thus will be the first experiment to investigate self-excited plasma dynamos. It will also allow the plasma viscosity to be varied independently of the conductivity, *i.e.,* the magnetic Prandtl number, P_m (the ratio of R_m to the hydrodynamic Reynolds number), to be varied from the liquid metal regime $P_m << 1$ to the regime $P_m >> 1$ that is thought to be important in many astrophysical situations. Such an experiment has never been performed, and yet simple extrapolations from existing multi-dipole confinement experiments show that it is feasible. Electrodes at the plasma edge will be biased to control the plasma flow, and the multi-dipole confinement will provide a large, unmagnetized region that has sufficiently high electron temperature, $T_e > 10$ eV, for the plasma to reach R_m of 1000. Changes in the ion species will allow the plasma viscosity to be varied such that P_m can be changed from values much less than unity to values much greater than unity. Once constructed, a variety of experiments can be carried out in the proposed facility, including campaigns investigating the following plasma processes: large scale dynamos; small scale dynamos; flow driven plasma turbulence; magnetorotational instabilities in plasmas; magnetic field line stretching; explosive reconnection; and, plasma instabilities at high beta and low collisionality.

4.3. NRL Space Physics Simulation Chamber

The Space Physics Simulation Chamber (SPSC) in the NRL PPD [19] currently produces plasmas scalable to ionospheric and magnetospheric conditions. Future capabilities are anticipated to produce plasmas better suited to study the physics of the solar corona.

The main SPSC chamber (Figure 13a) is 1.8-m in diameter, 5-m in length, and with a set of 5 independent magnetic field coils capable of producing a uniform magnetic field B of up to 250 G or other axisymmetric field geometries, including a diverging field. Typically argon plasmas are produced (other species have also been used) with a biased large area hot filament to generate a 0.75 m diameter magnetized plasma column with density range $n_e \sim 10^{5-11}/cm^3$, electron temperature $T_e \sim 0.5–2$ eV, and cold ions. These plasmas have been used for ionospheric plasma instability and ion energization experiments, space and laboratory diagnostic development, and most recently, for nonlinear whistler wave propagation studies [20–22].

Figure 13. a. The main NRL Space Physics Simulation Chamber (SPSC). b. Finite length Taylor double helix plasma (B_z isosurfaces) for a length over radius of 10.

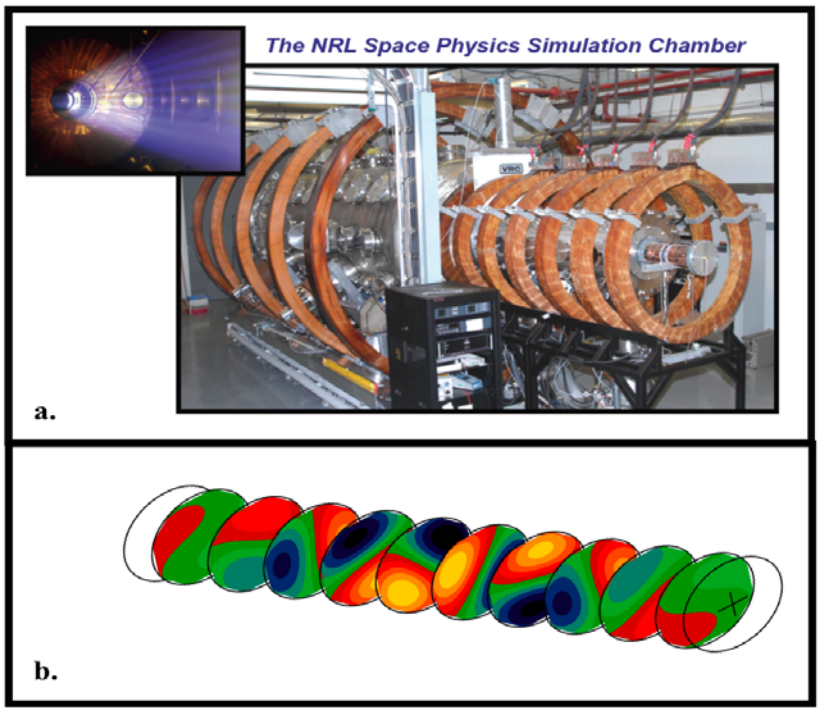

The SPSC source chamber, attached to the main chamber but independently operable, adds an additional 2-m of length with a smaller diameter of 0.55-m. Its magnetic coils permit up to a 1 kG solenoidal field. A radio frequency (RF) discharge is used to produce somewhat higher density plasmas but with a smaller range than the main chamber. Recent work has included investigations of ion cyclotron waves generated by sheared **E** × **B** flows, where 'E' denotes the electric field. This research could be extended to study the solar wind heating and acceleration problems by coupling the ion cyclotron wave generation experiment in the source chamber into the main chamber programmed with a diverging magnetic field geometry. The full ion velocity distribution function could then be measured where the experimental 'wind' should be generated, using a laser-induced fluorescence diagnostic that is now under construction, thus permitting spatially resolved flow as well as parallel and perpendicular ion temperature measurements.

Additional solar-relevant experiments are possible by making use of the properties of helical Taylor relaxed states [47]. These states roughly resemble a closed loop of flux that has been squeezed to fit inside a long cylindrical conducting boundary, then twisted with a pitch that asymptotically reaches a helical wave number of kR = 1.23 for very elongated cylinders, where k is the wavenumber and R is the radius; see Figure 13b. Plasma conditions B~1 kG, T_e, T_i both 10–20 eV, and $n_e \sim 10^{14}/cm^3$ are easily achieved using coaxial magnetized plasma gun sources. This helical plasma produced inside an open-ended cylindrical boundary in the source chamber of the SPSC would subsequently expand out into the main chamber of the SPSC in a manner similar to the propagation of a CME through interplanetary space. Once this expansion is characterized, and proven reproducible, a reconnection experiment utilizing two such loops of magnetized plasmas expanding toward one another would be feasible.

Finally, it may be possible to study MHD turbulence during SPSC plasma relaxation from an initial state containing multiple spheromaks (plasmoids) produced by two or more coaxial magnetized plasma gun sources. The dynamics evolving the multiple plasmoid initial state, with a short scale length, to the final relaxed state of the finite length Taylor double helix, with a longer characteristic length scale, may resemble an inverse cascade process. Taylor relaxation theory only stipulates helicity conservation as the plasma dissipates magnetic energy; it makes no precondition on the nature of the relaxation process itself. However, Taylor originally envisioned a turbulent relaxation process such that magnetic energy was dissipated effectively on short spatial scales [48]. Such an experiment would complement the large body of solar wind turbulence measurements and numerical simulations.

4.4. MIT Versatile Toroidal Facility

The MIT Versatile Toroidal Facility (VTF), Figure 14, provides direct and well-diagnosed experimental observation of spontaneous reconnection dynamics [28]. In this experiment a plasma parameter regime of special interest can be achieved where the reconnection process appears in rapid bursts. This regime provides a unique opportunity to study the scientifically unresolved 'trigger problem' of magnetic reconnection in current sheets. The most recent experiments document how the onset phase involves three-dimensional (3D) dynamics. The measurements include the detailed time evolution of the plasma density, current density, the magnetic flux function, the electrostatic potential and the reconnection rate. Reconnection is observed to start at one toroidal location, and then to propagate around the toroidal direction at the Alfvén speed calculated with the strength of the dominant guide magnetic field [49].

Figure 14. The MIT Versatile Toroidal Facility (VTF).

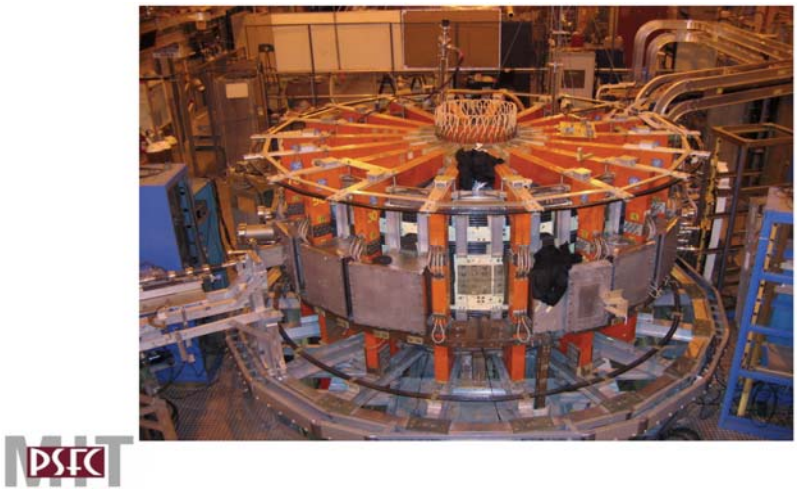

4.5. Swarthmore Spheromak Experiment

The Swarthmore Spheromak Experiment (SSX), which provides well-diagnosed data on 3D null-point magnetic reconnection that is also applicable to solar active regions embedded in pre-existing coronal fields. The SSX device [50] is cylindrically symmetric about the horizontal axis; see Figure 15. Spheromak plasmas are formed in the guns on the east and west sides of the vacuum chamber and ejected into the main flux conserver. The lines of sight of the monochrometer, the four-channel

soft X-ray array, and the ion Doppler spectrometer are at the midplane, aligned with the short axis of the chamber and perpendicular to the long axis, as indicated schematically by white squares in the Figure. Arrays of six magnetic probes, indicated with black lines in the Figure, obtain data of the evolving plasma. The plasma contoured in the Figure represents that of a field reversed configuration, which is the plasma structure that naturally forms when two counterhelicity spheromaks merge.

Figure 15. The Swarthmore Spheromak Experiment (SSX).

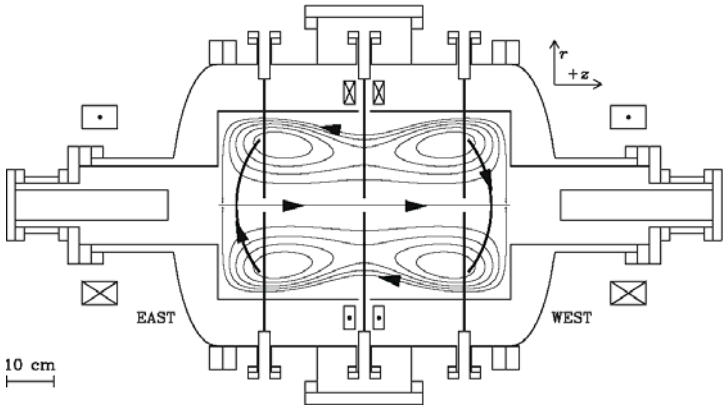

5. Examples of Developing Theoretical and Simulation Capabilities

New theoretical and simulation capabilities highlighted here, which provide world-leading numerical tools for the investigation of heliophysics and laboratory plasma experiments independently, and also bring a powerful, bridging computational basis for the synergistic research that is the focus of this review, include: HYPERION, a fully compressible 3D MHD code with radiation transport and thermal conduction; ORBIT-RF, a 4D Monte-Carlo code for the study of wave interactions with fast ions embedded in background MHD plasmas; the 3D implicit multi-fluid MHD spectral element code, HiFi; the 3D Hall MHD code VooDoo; and, the erupting flux rope (EFR) theoretical model. An overview of some relevant examples of MHD production codes–ARMS, CRUNCH, MHDCHAN, MHDFSL, and PHAETHON–is also presented.

5.1. HYPERION

In order to perform the MHD turbulence problem correctly with direct numerical simulation, it is necessary to resolve enough spatial scales to obtain an energy containing range, an inertial range, and a dissipation range with accuracy sufficient for computing inverse cascade [43] dynamics. Because of storage needs, the more that the complexity of the physical problem is reduced, the more spatial scales are obtainable. Hence most previous research in MHD has been restricted to dynamical effects, e.g., reduced MHD (or, the Strauss equations [43]), and cold plasma models. Incompressible and cold plasma models only contain the first few parts of the complete energy cycle, *i.e.,* magnetic energy creation through footpoint motions and energy conversion by means of magnetic reconnection. With these models, the physics involved with thermal conduction and radiation transport is neglected, and any magnetic energy lost through Ohmic diffusion and any kinetic energy lost through viscous diffusion is simply ignored by the computation and thus lost from the modeled system.

However, as computers are advancing, it is becoming more feasible to perform large-storage fully compressible magnetized plasma problems and model the complete energy cycle with good spatial resolution. The additional complexity of full compressibility is important for three categories of interest with respect to solar active region loops and the coronal heating problem: structural, dynamical, and thermodynamical.

HYPERION [26] is a 3D parallelized Fourier collocation–finite difference code with third order Runge-Kutta discretization that solves the compressible MHD equations with vertical thermal conduction and radiation included. This new tool is enabling investigation of the full Parker coronal heating model [51]. The most significant structural effect that HYPERION model includes is stratification due to gravity. The code can also modify the gravitational term to model the curvature of a typical loop. Among new dynamical effects that are possible are compression and rarefaction of the plasma, as well as formation of shocks. Thermodynamical effects include thermal conduction and optically thin radiation transport. In addition, the diffusivities can be temperature dependent. It is important to include these features in the model in order to begin to reproduce the complete energy cycle. Kinetic energy in the photosphere is transformed into magnetic energy in the corona by means of photospheric footpoint convection. Magnetic energy is then transformed into thermal (and kinetic, and perturbed magnetic) energy by means of magnetic reconnection in the corona. Heat is then conducted from the high temperature corona back toward the low temperature photosphere, where it is removed via radiation. HYPERION self-consistently calculates and tracks the optically thin radiation, enabling direct comparison with experimental observables.

HYPERION simulation results preserve the spatial intermittency of the kinetic and magnetic energies observed in earlier Parker-regime coronal heating simulations, and also provide new information about the evolution of plasma internal energy, *i.e.*, we can now determine how the coronal plasma heats up as a consequence of photospheric convection of magnetic footpoints. The example simulation data shown in Figure 16 is of a coronal loop turbulent compressible magnetofluid, the footpoints of which are being convected by random photospheric motions.

Figure 16. HYPERION results for a coronal loop whose line-tied magnetic field is being convected by random footpoint motions. Left: Loop energies *vs.* time in Alfvén units (left), where e_V is the kinetic energy, e_B is the magnetic energy, and E_{int} is the internal energy. Right: Dissipation *vs.* time in Alfvén units, where is the coronal loop enstrophy, J is mean-squared current, and D denotes the loop radiation losses.

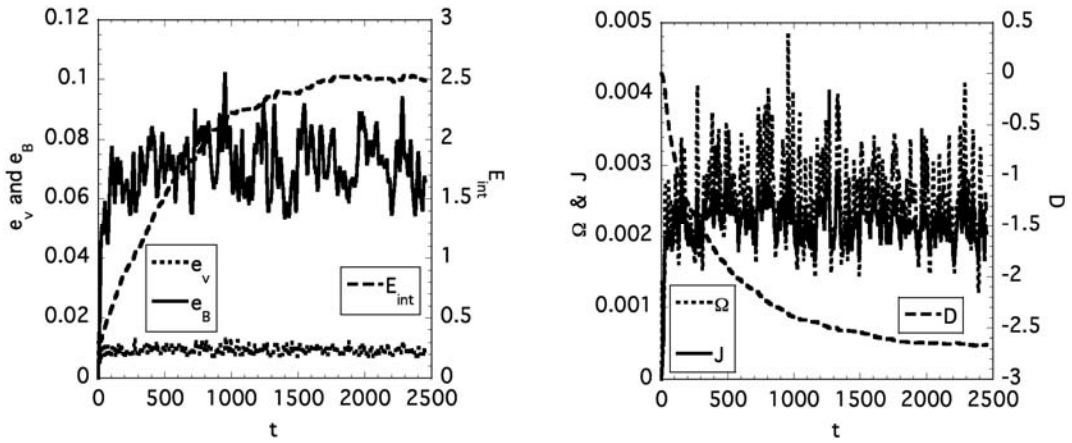

5.2. ORBIT-RF

ORBIT-RF is a new 4D Monte-Carlo code that is applicable to the study of wave interactions with fast ions embedded in background MHD plasmas. Several questions are of interest in space plasmas regarding the mechanism(s) for ion heating and acceleration in converging or diverging magnetic flux tubes. What is the origin of the ion cyclotron wave? How does a cyclotron wave selectively heat ions of different masses? What causes acceleration of the fast ion energy in the direction parallel to the magnetic field? The ORBIT-RF Monte-Carlo approach to modeling ion cyclotron wave heating of energetic ions in laboratory plasmas coupled to a full wave code for Alfvén/magnetosonic wave propagation is appropriate for studying these questions in space plasmas.

The Monte-Carlo approach reproduces the quasilinear (Q-L) physics but removes the two key restrictions to the standard model, zero ion drift orbits and uniform wave-particle interaction time, as both are not justified for energetic ions. It starts from a Fokker-Planck Q-L equation, derived from a gyrokinetic Vlasov equation [52]. The Q-L diffusion coefficient in the equation as a function of the electromagnetic wave fields is related to the 'kick' in velocity a particle receives as it goes through a cyclotron resonance, which is used to form a stochastic or Monte-Carlo (MC) equation. Coulomb collisions can be similarly implemented and the code can be easily parallelized on a massively parallel processing computer. The Monte-Carlo code ORBIT-RF is developed and being applied to the study of ion cyclotron RF (ICRF) wave accelerations of fast ions in tokamaks [53].

In ORBIT-RF, the unperturbed motion of an ion is solved using Hamiltonian equations of guiding center drifts. In this lowest drift ordering, the magnetic moment μ is a constant of motion, so the guiding-center equations are solved in 4D making the code very efficient. In the next order, the magnetic moment is no longer conserved. The change in μ that has a mean component and a random component reflecting the random walk diffusive process is obtained from the MC equation. It is non-zero only when close to the cyclotron resonance and the width of the resonance is related to the interaction time. Presently, ORBIT-RF has kept only the dominating change in velocity space, which is in μ, and has neglected changes in spatial diffusion and parallel velocity due to the RF waves. The contribution of the parallel wave electric field is similarly neglected. For space plasma applications, the parallel acceleration by the wave electric field may be important and should be retained.

The wave absorption model has been benchmarked against linear full-wave zero orbit-width predictions from the Fokker-Planck/full-wave code CQL3D/AORSA for various ion cyclotron harmonics. Systematic comparisons performed with an initial iteration for a Maxwellian plasma largely reproduce linear absorption directly evaluated by the AORSA dielectric tensor. Iterations between ORBIT-RF and AORSA to update the non-Maxwellian dielectric tensor, which in turn is used to update the wave electric field, suggest qualitative differences in the spatial absorption location and the fast ion energy spectrum.

ORBIT-RF has also been validated with experiments. Comparison with Alcator C-Mod fundamental heating data shows agreement with the measured minority ion energy distribution, as well as with Stix's [54] analytic formula. Another comparison is with the DIII-D 4^{th} and 8^{th} harmonics heating data. ORBIT-RF calculated a stronger absorption for the 4^{th} harmonic than for the 8^{th} harmonic. Furthermore, it produced a larger tail for the 4^{th} harmonic with only half the power (Figure 17). Both observations are consistent with experiments but not with linear theory.

Figure 17. Energetic ion distribution accelerated by high harmonic on ion cyclotron RF (ICRF) waves.

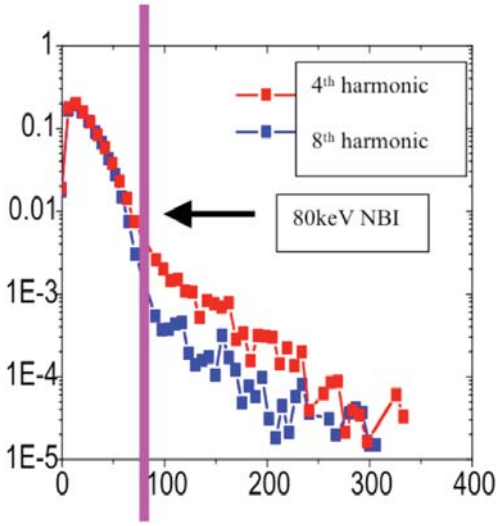

To include flux converging/divergent features important for space plasmas, ORBIT-RF will need to be adapted to a 3D magnetic equilibrium geometry. A separate code (if such a code exists for space plasmas) can be used to evaluate the cyclotron wave instabilities and calculate the cyclotron wave structure, similar to the use of the full wave code AORSA; and, ORBIT-RF will use that information to calculate the ion acceleration for different ion species. The result can be use to validate against observations. Alternatively, we can start with the original gyrokinetic equation [52], solving the 1st order high frequency equation for wave propagation and instability, and the next order drift-orbit equation for wave heating and particle acceleration. Specifically this approach may be applicable for studying acceleration of heavier ions in space plasmas by Alfvén waves whose frequency is below the cyclotron frequency of the lightest ion.

5.3. HiFi

HiFi is a user-friendly highly parallel fully implicit adaptive spectral element code framework designed for model development and multi-fluid numerical modeling in two- and three-dimensional geometries [55,56]. HiFi capabilities continue to be expanded and improved, with operational and well-tested code versions having been released under a BSD (Berkeley Software Distribution) style license.

One of the key features of HiFi is the very general 'flux-source' form of the system of partial differential equations (PDEs), which can be solved by the code [55,56]. Together with an equally general formulation of allowable boundary conditions and the modular structure of the code, the HiFi framework provides a capable tool for development, verification and validation of multi-fluid plasma models. The combination of a user-friendly interface structure with minimal overhead and the state-of-the-art numerical methods designed to allow the code to run on modern massively parallel computers is the hallmark of the HiFi framework.

High-order spectral element representation is used in HiFi in all spatial dimensions to take advantage of an exponentially convergent spatial discretization error, while the discretization operator remains localized and therefore amenable to massive parallelization. The spectral element

representation also allows modeling topologically and geometrically complex physical domains, characteristic of laboratory plasmas. An available grid adaptation algorithm then enables the code to re-map the grid, as necessary, whenever fine scale structures – particularly prominent in systems where magnetic reconnection takes place–dynamically arise and begin to require higher resolution anywhere within the domain. This feature, called static r-refinement of the mesh, allows the grid points to be automatically moved in physical space whenever desired in order to approximately equidistribute the spatial convergence error of the solution; and, an additional feature allows the mesh surfaces to be aligned with a locally preferred direction.

Many laboratory and heliospheric plasmas cannot be accurately described by the single-fluid MHD approximation. Instead, extension to a two-fluid or a collisionless description of the plasma becomes necessary. PDEs associated with such systems usually possess time-scales which are much faster than those of dynamical interest in numerical modeling of the plasmas, while the stability criteria for an explicit time-advance require adhering to a stringent Courant-Friedrichs-Lewy (CFL) condition forcing the time-step to correspond to the fastest possible wave in the system. An implicit time-advance avoids this restriction, limiting the time-step size to accuracy considerations. In HiFi, fully implicit adaptive time-advance allows large time-steps whose size is limited only by the dynamical time-scales present in the domain at each particular time.

The HiFi framework has already been used to address a number of computational problems both in two and three dimensions. In a recent application, HiFi was used to model the interaction between two spheromaks in a laboratory plasma, as shown in Figure 18 [6].

Figure 18. HiFi simulation of two interacting 3D magnetic structures, called spheromaks. Shown are streamlines of magnetic field as the two spheromaks tilt and reconnect through a localized region containing a magnetic null (left panel), merging into a single helical structure (right panel). Magnetic field vectors in the $\varphi = \pm\pi/2$ plane are shown in the left panel. Successful comparison of the simulation with the SSX experimental data has been performed [6].

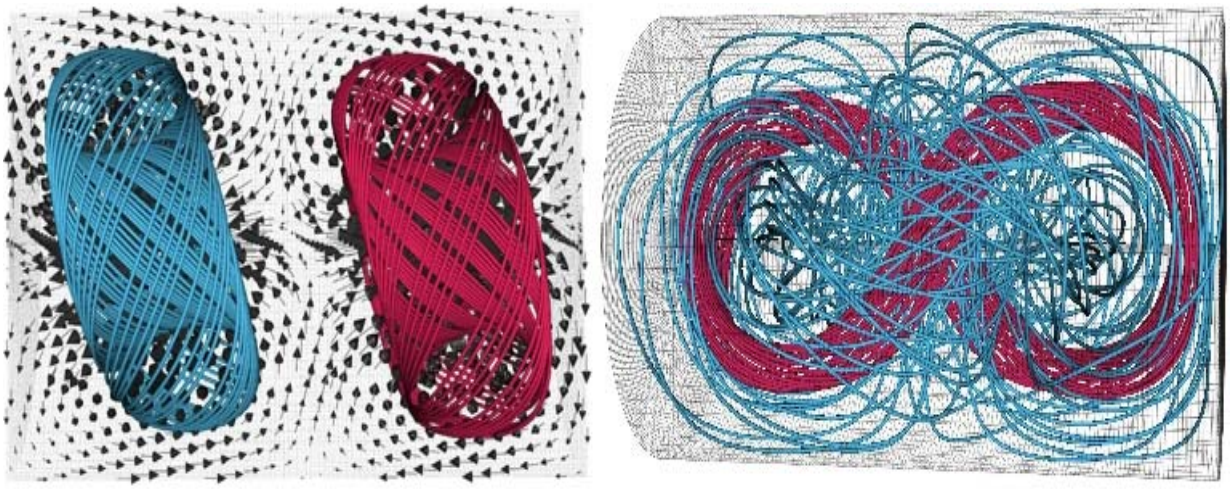

In a collaboration between NRL SSD and the experimental team of the SSX device (see Section 4.5), the first complementary numerical simulation and experimental observation of 3D

null-point magnetic reconnection and subsequent dynamical relaxation to a 3D helical lowest energy state have been obtained. These results indicate that significant amounts of energy should be readily available for fast release via magnetic reconnection in similarly complex solar magnetic configurations created by the emergence of new solar active regions into pre-existing coronal fields. They also demonstrate the capability of the modern computational tools, such as HiFi, to model the fundamental dynamics of these systems.

5.4. VooDoo

The NRL 3D Hall MHD code VooDoo [57] is used to perform simulations in which Hall physics can play a critical role in the magnetic reconnection process. The Hall term decouples the ion and electron motion on scale lengths less than an ion inertial length, and is important for plasma dynamics on length scales less than the ion inertial length but greater than the electron inertial length, and time scales shorter than an ion cyclotron period. A significant difference when the Hall term is included into MHD reconnection dynamics is the development of an 'out of plane' magnetic field. This component of the wave field is associated with the generation of a whistler wave. Figure 19 shows 3D consequences of the Hall reconnection process on the (initially 2D) plasma flow. The plasma initially flows toward the midplane, but as one moves away from the reconnection X-point the plasma flow fans out, and the reconnecting field lines appear to 'whip' the plasma towards the magnetic O-points as they release their tension.

Figure 19. VooDoo simulation of Hall MHD reconnection. Left: Magnetic field streamlines at z = 0. Right: Flow velocity streamlines, at the same time and position.

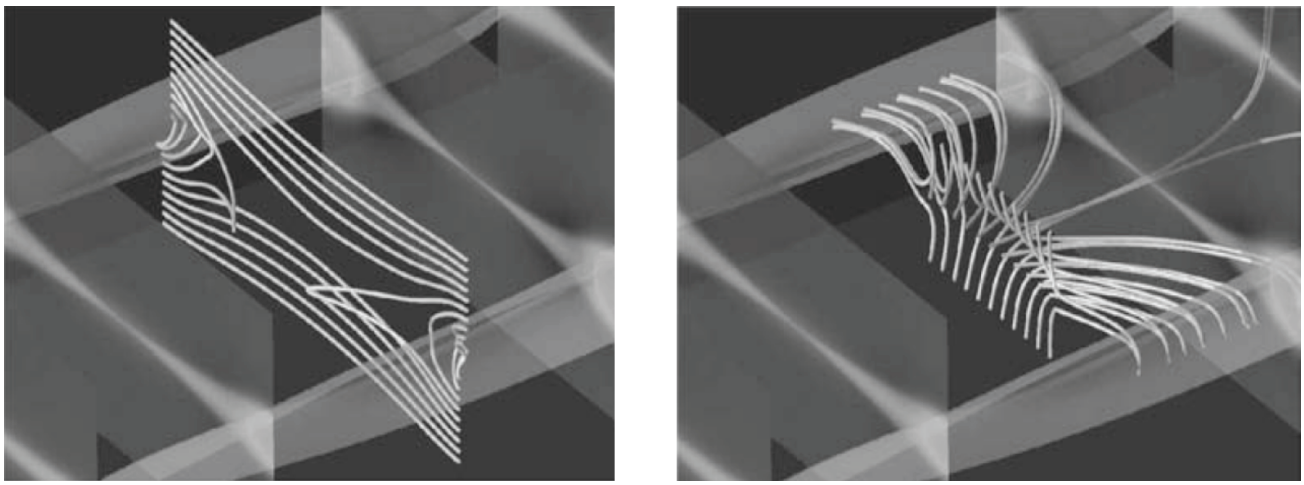

5.5. Theoretical Model of CMEs: The Erupting Flux Rope (EFR) Model

A fundamental outstanding question in CME physics is the driving mechanism. In this respect, the NRL's erupting flux rope (EFR) model of CMEs [58,59] has been shown to correctly reproduce observed CME trajectories within the LASCO [60] field of view (30 solar radii). It has been extensively tested and validated using the SOHO [61] data showing excellent agreement [62–64]. This theoretical model is based on the hypothesis that the magnetic field underlying a CME is that of a magnetic flux rope with quasi-stationary photospheric footpoints. The driving force in this model is the

Lorentz hoop force, originally derived by Shafranov [65] for axisymmetric toroidal equilibria. Application of Shafranov's work to a nonaxisymmetric dynamical system requires essential modifications. In particular, the presence of the stationary footpoints for CMEs introduces spatial and temporal scales that are absent in axisymmetric configurations. An important discovery based on the EFR model is the separation distance between the footpoints of the flux rope governs the CME acceleration profiles and is directly manifested in observed CME acceleration [66]. Such observed scales are fundamental to testing theoretical and numerical models [67] as well as formulating laboratory simulations of the CME phenomena.

5.6. ARMS, CRUNCH, MHDCHAN, MHDFSL and PHAETHON

In addition to the new or developing simulation codes described above, much ongoing research is being performed with MHD production codes, which would greatly enhance and also benefit from the synergistic research that is the subject of this paper. In this Section we briefly highlight a few of these computational capabilities, as illustration.

The ARMS code [68] is a Flux-Corrected Transport (FCT) based [69] adaptive mesh computational capability that simulates a range of solar and coronal problems. The code was recently successfully applied to the problem of patchy reconnection in a Y-type current sheet [70], as shown in Figure 20. This simulation addressed the question of how magnetic reconnection has the near-simultaneous effects that are observed over very large scales (on the Sun, 10^7-m), if it must occur on small (10-m) scales in order to be sufficiently fast to explain the timescales of the solar flare observations. In some flares, it appears that reconnection starts at a few isolated points in the current sheet, as evidenced by the point-like nature of the initial footpoint brightening in those flares. Yet soon after these isolated footpoints light up, the footpoint emission quickly extends so that a pair of nearly continuous, parallel lines, or ribbons, lights up in the chromosphere. These two lines lie on either side of the polarity inversion line of the vertical magnetic field below the current sheet, indicating that they represent the two footpoints of the newly reconnected fieldline loops. This rapid generation of flare ribbons indicates that the initial, localized, reconnection in the coronal current sheet has quickly extended such that a large portion of the current sheet is simultaneously reconnecting. These two ribbons then separate from each other, consistent with the interpretation that magnetic flux is being processed through the reconnection site with flux which was initially farther from the reconnection site, and which therefore has footpoints successively farther from the polarity inversion line, being processed at successively later times. So far, the simulation results such as displayed in Figure 20 rely on untested numerical effects. It would be of profound importance to study the VTF results that are described in Sections 2.1 and 4.4, from the perspective of these simulation results, or to reproduce experimental results from the MRX (Magnetic Reconnection Experiment) [71] at the Princeton Plasma Physics Laboratory.

The 3D MHD triply periodic compressible collocation code, CRUNCH [72], was initially developed to investigate reconnection of magnetic fluxtubes at various contact angles, as shown in Figure 21. It has been applied to a wide range of plasma dynamics problems, including the relaxation of solar coronal plasmas to force free states.

The Fourier pseudospectral Chebyshev collocation channel code with no-slip boundary conditions, MHDCHAN [73], and the related free-slip boundary conditions code, MHDFSL [74], are being applied to a broad range of magnetohydrodynamics problems that are relevant to solar coronal and laboratory plasmas. Figure 22 illustrates MHDCHAN simulations of the University of Texas at Austin (UT-Austin) Helimak evolution (left) and of the MHD secondary instability that may provide explanation for the fast reconnection timescales that are observed in solar magnetic reconnection with MHDFSL [75] (right).

PHAETHON [27] is a highly parallelized 3D cold plasma MHD code that is spectrally periodic in the (X,Y) cross plane and has line-tied boundary conditions in the vertical (Z) direction. Space is discretized with a Fourier collocation scheme in X and Y, and a staggered grid finite difference scheme is used in Z. Time is discretized with a low storage Runge-Kutta method. PHAETHON is being used to investigate solar coronal heating for coronal loops that are line-tied to the photosphere, as illustrated in Figure 23. PHAETHON has been crucial in demonstrating the importance of explosive instabilities in coronal heating [27].

Figure 20. ARMS MHD simulation of solar flare reconnection in a Y-type current sheet, with time increasing from (a) through (f). Magnetic reconnection is initiated by a localized sphere of enhanced resistivity on the current sheet, high in the solar corona. Reconnected loops retract down to the low corona, coming to rest on the pre-existing arcade of loops. This arcade builds up as more magnetic flux reconnects above it, in agreement with observations. The simulation also shows the propagation of reconnection to the left and right of the initial reconnection site, as is observed in the corona, though here the propagation is due to artificial numerical effects [68].

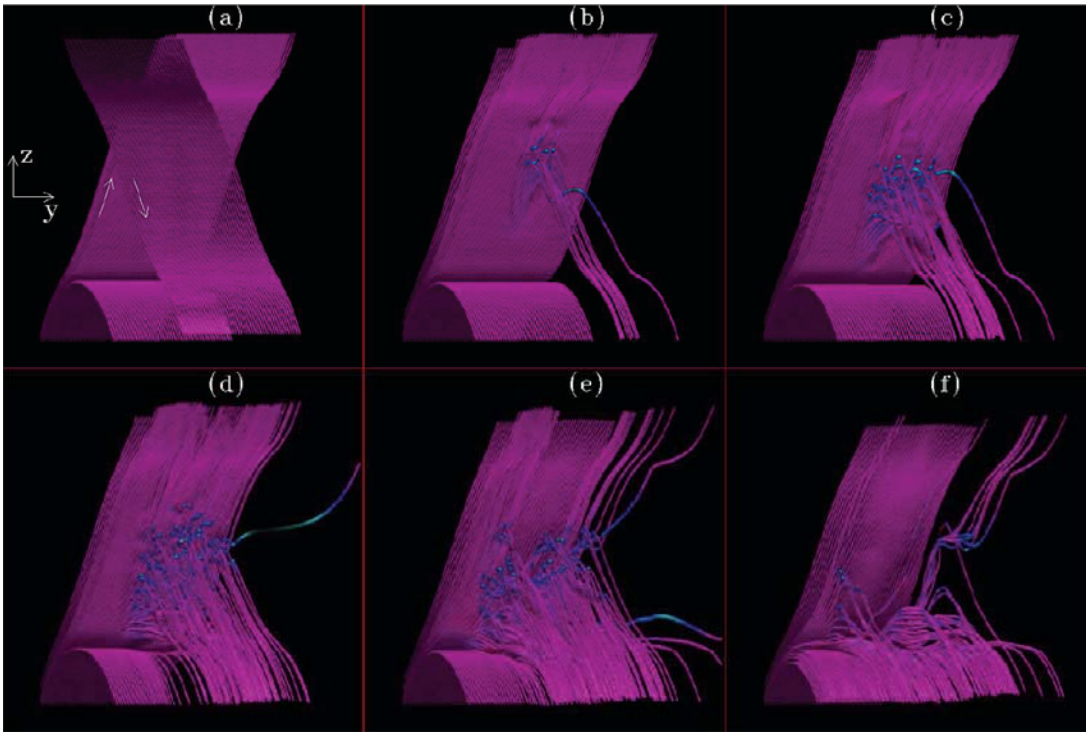

Figure 21. CRUNCH 3D compressible MHD simulation of fluxtube tunneling. Note that fluxtubes pass through each other as multiple field line reconnections occur.

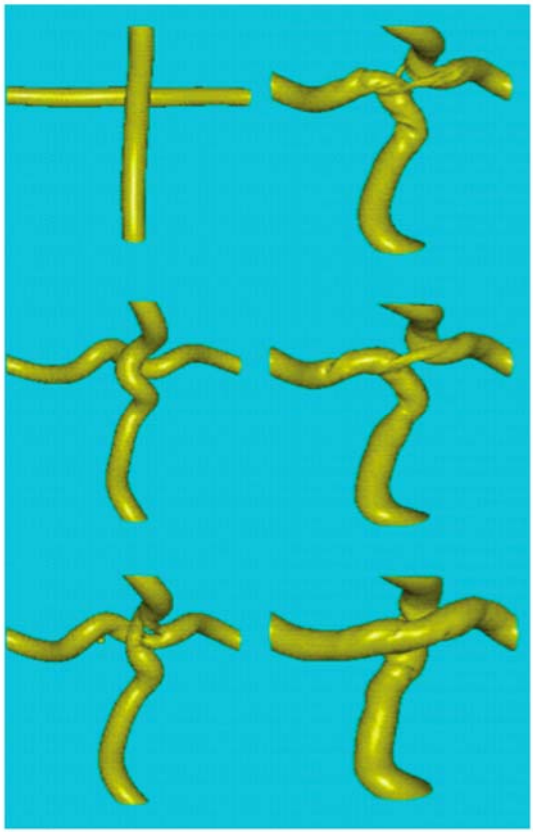

Figure 22. Left: MHDCHAN 3D MHD simulation of the UT-Austin Helimak evolution. Vorticity isosurfaces and some streamlines are shown. Right: MHDFSL 3D simulation of the secondary instability that may provide explanation for the fast observed solar magnetic reconnection timescales. A late stage plasma current configuration is shown.

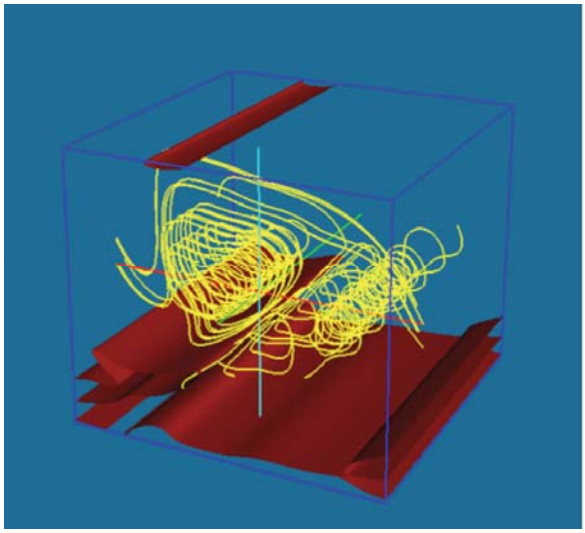

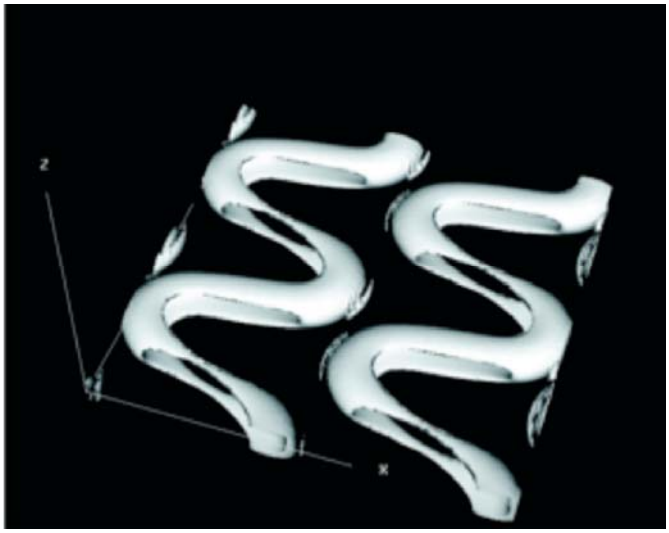

Figure 23. PHAETHON 3D MHD simulation. Left: Vertical current isosurfaces and sample magnetic field lines in a random force coronal heating simulation. Right: Current isosurfaces and representative magnetic field lines during a line-tied explosive instability calculation.

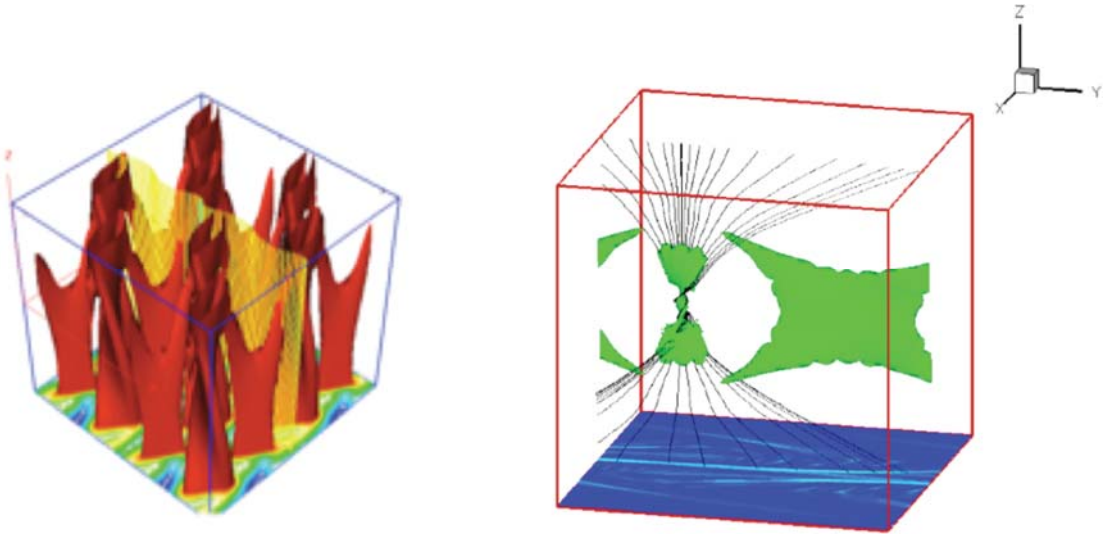

6. Summary

Many scientific and technical questions of considerable merit can be addressed by collaborations among researchers and capabilities from the two distinct disciplines of heliophysics and laboratory plasma physics. We summarize four areas that we have identified in this review as most promising, as immediate next steps, as follows:

First, loop dynamics by observations, laboratory experiments in cylindrical or toroidal geometry, and simulations, to investigate open questions pertaining to magnetic reconnection, and plasma dynamics and instabilities, such as:

- How can a loop hold plasma? Does it do so, *i.e.*, is a 'loop' a real construct?
- What is the fundamental solar loop geometry: a coherent hoop that may go unstable as it is twisted, or strands that reconnect in passing?
- How do details of embedded and surrounding magnetic geometry, such as the presence (or absence) of a loop guide magnetic field, affect loop dynamics?
- How is reconnection triggered in open field geometries (solar conditions) as compared with closed field geometries (most laboratory conditions)?
- What are the physical scales of magnetic reconnection in the solar corona? How does reconnection scale from laboratory to the corona?
- What are the physical scales governing the dynamics of expanding flux ropes?
- Does fundamental loop geometry (hoop or strand) affect the reconnection process?
- Does the presence (or absence) of parallel loop current affect the reconnection process?
- Is the physics of reconnection propagation along a solar flare arcade similar to the physics of reconnection propagation around a laboratory torus?

- Can the possible reconnection drivers for abundance anomalies (contracting magnetic islands as compared with a sawtooth instability) be discriminated in laboratory loop-like experiments?

Second, heliospheric dynamics by observations, laboratory experiments in slab or cylindrical geometry with a diverging magnetic field, and simulations, to investigate heliospheric open questions such as:

- How are ion cyclotron waves excited and under what conditions in the solar wind?
- Do ions propagating in a diverging magnetic field get accelerated (as a result of ion cyclotron wave absorption)?
- Can the ion cyclotron wave absorption mechanism account for plasma heating as the plasma passes through the heliosphere (which has as signature a larger than expected charge state at L1)?
- How do density fluctuations evolve as they propagate through the diverging magnetic field of the heliosphere: are they primarily passively advected, or is macroscopic turbulence generated?
- How do expanding flux ropes evolve while interacting with the ambient plasma medium?

Third, plasma atomics physics by observations, spectroscopy experiments in laboratory regimes, and simulations, to validate instruments and atomic modeling, and address open questions such as:

- Are the current solar radiation models accurate?
- How accurate are electron density diagnostic line ratios in ions such as Fe^{+11}, Fe^{+12}, *etc.*?
- How accurate are radiative decay rates in many ions of solar interest?
- How accurate are electron impact excitation rate coefficients in many ions of solar interest?

Fourth, dynamo physics primarily in spherical geometry laboratory experiments and simulations, to address open questions such as:

- How does a magnetic dynamo depend on the rotation rate?
- How does a magnetic dynamo depend on the depth of the convection zone?

Investigating and exploiting these heliophysics and laboratory plasma synergies will underpin the development of a more comprehensive and reliable predictive understanding of key plasma energy release and transport processes, which will greatly benefit both space and also fusion energy sciences.

Acknowledgements

This review was supported by the Naval Research Laboratory and the Office of Naval Research. Conversations with Thomas Mehlhorn (NRL PPD Superintendent) are gratefully acknowledged.

References

1. Howard, R.A. A historical perspective of coronal mass ejections. *Geophys. Mono. Ser.* **2006**, *165*, 7–13.
2. Doschek, G.A.; Warren, H.P.; Mariska, J.T.; Muglach, K.; Culhane, J.L.; Hara, H.; Watanabe, T. Flows and nonthermal velocities in solar active regions observed with the EUV imaging spectrometer on *Hinode:* A tracer of active region sources of heliospheric magnetic fields? *Astrophys. J.* **2008**, *686*, 1362–1371.

3. Doschek, G.A.; Landi, E.; Warren, H.P.; Harra, L.K. Bright points and jets in polar coronal holes observed by the extreme-ultraviolet imaging spectrometer on *Hinode. Astrophys. J.* **2010,** *710*, 1806–1824.
4. Phillips, K.J.H.; Feldman, U.; Landi, E. *Ultraviolet and X-ray Spectroscopy of the Solar Atmosphere;* Cambridge Astrophysics Series 44. Cambridge University Press: Cambridge, UK, 2008.
5. National Academies Space Studies Board. *Severe Space Weather Events–Understanding Societal and Economic Impacts: A Workshop Report;* National Academies Press: Washington, DC, USA, 2008; Available online: http://www.nap.edu/openbook.php?isbn=0309127696&page=R1 (Accessed on 6 May 2010).
6. Lukin, V.S.; Brown, M.R.; Cothran, C.D.; Gray, T. Three-dimensional null-point magnetic reconnection and relaxation. *Phys. Rev. Lett.* 2009, submitted.
7. Shimomura, Y; Aymar, R.; Chuyanov, V.; Huguet, M., Parker, R.; ITER Joint Central Team; ITER Joint Central Team and Home Teams. ITER overview. *Nucl. Fusion* **1999**, *39*, 1295–1308; also available online: http://www.iter.org (Accessed on 6 May 2010).
8. Dahlburg, J.; Allen, S.; Betti, R.; Knowlton, S.; Maingi, R.; Navratil, G.A.; Sabbagh, S.; Sheffield, J.; VanDam J.; Whyte, D. Characteristics and contributions of the three major United States toroidal magnetic fusion facilities. *J. Fusion Energ.* **2005**, *3–4*, 125–171.
9. *The STEREO Mission*; Russell, C.T., Ed.; Springer: New York, NY, USA, 2008.
10. *The Hinode Mission*; Sakurai, T., Ed.; Springer: New York, NY, USA, 2008.
11. SDO/Solar Dynamics Observatory. Available online: sdo.gsfc.nasa.gov/mission/science/science.php (Accessed on 6 May 2010).
12. IRIS/Interface Region Imaging Spectrograph. Available online: http://www.nasa.gov/home/hqnews/2009/jun/HQ_09-141_SMEX_Selections.html (Accessed on 6 May 2010).
13. Solar Orbiter. Available online: http://www.esa.int/esaSC/120384_index_0_m.html (Accessed on 6 May 2010).
14. Dahlburg, J.; Corones, J.; Batchelor, D.; Bramley, R.; Greenwald, M.; Jardin, S.; Krasheninnikov, S.; Laub, A.; Leboeuf, J.-N.; Lindl, J.; Lokke, W.; Rosenbluth, M.; Ross, D.; Schnack, D. Fusion Simulation Project: Integrated simulation and optimization of fusion systems. *J. Fusion Energ.* **2001**, *20*, 135–196.
15. NASA Heliophysics Roadmap, 2009 Heliophysics Roadmap Team; NASA: Washington, DC, USA, 2009; Available online: http://sec.gsfc.nasa.gov/sec_roadmap.htm (Accessed on 6 May 2010).
16. Baker, C.; Praeger, S.; Abdou, M.; Berry, L.; Betti, R.; Chan, V.; Craig, D.; Dahlburg, J.; Davidson, R.; Drake, J.; *et al.* Scientific challenges, opportunities and priorities for the U.S. Fusion Energy Sciences Program. *J. Fusion Energ.* **2005**, *1–2*, 13–114.
17. *Dialogues Concerning Two New Sciences*; Galilei, G., Ed.; Dover Publications Inc: New York, NY, USA; 1954.
18. Bushnell, D.M. Scaling: Wind tunnel to flight. *Ann. Rev. Fluid Mech.* **2006**, *38*, 111–128.
19. Amatucci, W.E.; Blackwell, D.D.; Walker, D.N.; Gatling, G.; Ganguli, G. Whistler wave propagation and whistler wave antenna radiation resistance measurements. *IEEE Trans. Plasma Sci.* **2005**, *33*, 637–646.
20. Blackwell, D.D.; Walker, D.N.; Messer, S.J.; Amatucci, W.E. Antenna impedance measurements in a magnetized plasma, I. Spherical antenna. *Phys. Plasmas* **2007**, *14*, Art. No. 092105.

21. Blackwell, D.D.; Walker, D.N.; Messer, S.J.; Amatucci, W.E. Antenna impedance measurements in a magnetized plasma, II. Dipole antenna. *Phys. Plasmas* **2007**, *14*, Art. No. 092106.
22. Blackwell, D.D.; Walker, D.N.; Amatucci, W.E. Whistler wave propagation in the antenna near and far fields in the Naval Research Laboratory Space Plasma Simulation Chamber. *Phys. Plasmas* **2010,** *17,* Art. No. 012901.
23. Linton, M.G. Dynamics of magnetic flux tubes in space and laboratory plasmas. *Phys. Plasmas* **2006**, *13*, Art. No. 058301.
24. Krall, J.; Chen, J. Density structure of a pre-eruptional coronal flux loop. *Astrophys. J.* **2005**, *628*, 1046–1055.
25. Murphy, R.J. Exploring solar flares with gamma rays and neutrons. *NRL Rev.* **2008**, *1*, 109–120; Available online: http://www.nrl.navy.mil/media/publications/nrl-review (Accessed on 21 May 2010).
26. Dahlburg, R.B.; Rappazzo, A.F.; Velli, M. Turbulence, energy transfers and reconnection in compressible coronal heating field-line tangling models. *Solar Wind* **2009**, *12*, e-print arXiv: 0912.1063.
27. Dahlburg, R.B.; Liu, J.-H.; Klimchuk, J.A.; Nigro, G. Explosive Instability and Coronal Heating. *Ap. J.* **2009**, *704*, 1059–1064.
28. Egedal, J.; Fox, W.; Katz, N.; Porkolab, M.; Reim, K.; Zhang, E. Laboratory observations of spontaneous magnetic reconnection. *Phys. Rev. Lett.,* **2007**, *98*, Art. No. 015003.
29. Lin, R.P.; Krucker, S.; Hurford, G.J.; Smith, D.M.; Hudson, H.S.; Holman, G.D.; Schwartz, R.A.; Dennis, B.R.; Share, G.H.; Murphy, R.J.; Emslie, A.G.; Johns-Krull C.; Vilmer, N. *RHESSI* observations of particle acceleration and energy release in an intense solar gamma-ray line flare. *Astrophys. J.* **2003**, *595*, L69–L76.
30. Laming, J.M. Non-WKB models of the first ionization potential effect: implications for solar coronal heating and the coronal helium and neon abundances. *Astrophys. J.* **2009**, *695*, 954–969.
31. Laming, J.M. On collisionless electron-ion temperature equilibration in the fast solar wind. *Astrophys. J.* **2004**, *604*, 874–883.
32. Laming, J.M.; Lepri, S.T. Ion charge states in the fast solar wind: new data analysis and theoretical refinements. *Astrophys. J.* **2007**, *660*, 1642–1652.
33. Habbal, S.R.; Druckmuller, M.; Morgan, H.; Daw, A.; Johnson, J.; Ding, A.; Arndt, M.; Esser, R.; Rusin, V.; Scholl, I. Mapping the distribution of electron temperature and Fe charge states in the coronal with total solar eclipse observations. *Astrophys. J.* **2010**, *708*, 1650–1662.
34. Kataoka, R.; Ebisuzaki, T; Kusano, K.; Shiota, D.; Inoue, S.; Yamamoto, T.T.; Tokumaru, M. Three-dimensional MHD modeling of the solar wind structures associated with 13 December 2006 coronal mass ejection. *J. Geophys. Res.* **2009**, *114*, Art. No. A10102.
35. Carter, T.A.; Brugman, B.; Pribyl, P.; Lybarger, W. Laboratory Observation of a Nonlinear Interaction between Shear Alfven Waves. *Phys. Rev. Lett.* **2006**, *96*, 1555001–1555005.
36. Doschek, G.A.; Feibelman, W.A. An improved spectral line list for the symbiotic star RR telescopii. *Astrophys. J. Suppl. Ser.* **1993**, *87*, 331–336.
37. Laming, J.M.; Titarchuk, L. Outflows near an accreting black hole: ionization and temperature structures. *Astrophys. J.* **2004**, *615*, L121–L124.

38. Withbroe, G.L.; Kohl, J.L.; Weiser, H.; Munro, R.H. Probing the solar wind acceleration region using spectroscopic techniques. *Space Sci. Rev.* **1982**, *33*, 17–52.
39. Brown, C.M.; Feldman, U.; Doschek, G.A.; Seely, J.F.; La Villa, R.E.; Jacobs, V.L.; Henderson, J.R.; Knapp, D.A.; Beiersdorfer, P.; Levine, M.A. Measurement of relative electron-impact-excitation cross sections for Fe^{24+}. *Phys. Rev. A* **1989**, *40*, 4089–4092.
40. Henderson, J.R.; Beiersdorfer, P.; Bennett, C.L.; Chantrenne, S.; Knapp, D.A.; Marrs, R.E.; Schneider, M.B.; Wong, K.L.; Doschek, G.A.; Seely, J.F.; Brown, C.M.; La Villa, R.E.; Dubau, J., Levine, M.A. Polarization of x-ray emission lines from heliumlike scandium as a probe of the hyperfine interaction. *Phys. Rev. Lett.* **1990**, *65*, 705–708.
41. Laming, J.M.; Kink, I.; Takacs, E.; Porto, J.V.; Gillaspy, J.D.; Silver, E.H.; Schnopper, H.W.; Bandler, S.R.; Brickhouse, N.S.; Murray, S.S.; Barbera, M.; Bhatia, A.K.; Doschek, G.A.; Madden, N.; Landis, D.; Beeman, J.; Haller, E.E. Emission-line intensity ratios in Fe XVII observed with a micro-calorimeter on an electron beam ion trap. *Ap. J.* **2000**, *545*, L161–L164.
42. Nandy, D. Outstanding issues in solar dynamo theory. In *Magnetic Coupling between the Interior and the Atmosphere of the Sun*; Hasan, S.S., Rutten, R.J., Eds.; Springer-Verlag: Heidelberg, Berlin, 2009. (to appear)
43. Montgomery, D.C. Major disruptions, inverse cascades, and the Strauss equations. *Phys. Scr.* **1982**, *T2/1*, 83–88.
44. Liu, Y.; Davies, J.A.; Luhmann, J.G.; Vourlidas, A.; Bale, S.D.; Lin, R.P. Geometric triangulation of imaging observations to track coronal mass ejections continuously out to 1 AU. *Astrophys. J.* **2010**, *720*, 82–87.
45. Bergerson, W.F.; Forest, C.B.; Fiksel, G.; Hannum, D.A.; Kendrick, R.; Sarff, J.S.; Stambler, S. Onset and saturation of the kink instability in a current-carrying line-tied plasma. *Phys. Rev. Lett.* **2006,** *96*, Art. No. 015004.
46. Spence, E.J.; Reuter, K.; Forest, C.B. A spherical plasma dynamo experiment. *Astrophys. J.* **2009,** *700,* 470–478.
47. Cothran, C.D.; Brown, M.R.; Gray, T.; Schaffer, M.J.; Marklin, G. Observation of a helical self-organized state in a compact toroidal plasma. *Phys. Rev. Lett.* 2009, *103*, Art. No. 251002.
48. Taylor, J.B. Relaxation of toroidal plasma and generation of reverse magnetic fields. *Phys. Rev. Lett.* **1974**, *33*, 1139–1141.
49. Katz N.; Egedal, J.; Fox, W.; Le, A.; Bonde, J.; Vrublevskis, A. Laboratory observation of localized onset of magnetic reconnection. **2010**, *Phys. Rev. Lett.*. (submitted)
50. Chaplin, V.H.; Brown, M.R.; Cohen, D.H.; Gray, T.; Cothran, C.D. Spectroscopic measurements of temperature and plasma impurity concentration during magnetic reconnection at the Swarthmore Spheromak Experiment. *Phys. Plasmas* **2009**, *16*, Art, No. 042505.
51. Parker, E.N. Magnetic neutral sheets in evolving fields, II, formation of the solar corona. *Astrophys. J.* **1983**, *264*, 642–647.
52. Chiu, S.C.; Chan, V.S.; Lin-Liu, Y.R.; Omelchenko, Y. Gyrokinetic Theory in the White-Chance-Boozer Coordinates. *Phys. Plasmas* **2000**, *7*, 4609–4615.
53. Choi, M.; Chan, V.S.; Berry, L.A.; Jaeger, E.F.; Green, D.; Bonoli, P.; Wright, J.; RF Scidac Team. Comparison of Monte-Carlo Ion Cyclotron Heating Model with Full-Wave Linear Absorption Model. *Phys. Plasmas* **2009**, *16*, Art, No. 052513.

54. Stix, T.H. *Waves in Plasmas.* American Institute of Physics: New York, NY, USA, 1992.
55. Lukin, V.S.; Glasser, A.H.; Lowrie, W; Meier, E.T. Overview of HiFi–implicit spectral element code framework for general multi-fluid applications. *J. Comput. Phys*. 2009; submitted.
56. Lukin, V.S. *Computational study of the internal kink mode evolution and associated magnetic reconnection phenomena*. Ph.D. thesis, Princeton University, **2007**.
57. Huba, J.D. Hall magnetohydrodynamics–a tutorial. In *Space Plasma Simulation*, Buchner, J., Dum, C.T., Scholer, M., Eds.; Springer-Verlag: Berlin Heidelberg, Germany, 2003; 166–192, LNP 615.
58. Chen, J. Effects of toroidal forces in current loops embedded in a background plasma. *Ap. J.* **1989,** *338*, 453–470.
59. Chen, J. Theory of prominence eruption and propagation: Interplanetary consequences. *J. Geophys. Res.* **1996**, *101*, 27499–27519.
60. Brueckner, G.E.; Howard, R.A.; Koomen, M.J.; Korendyke, C.M.; Michels, D.J.; Moses, J.D.; Socker, D.G.; Dere, K.P.; Lamy, P.L.; Llebaria, A.; Bout, M.V.; Schwenn, R.; Simnett, G.M.; Bedford, D.K.; Eyles, C.J. The Large Angle Spectroscopic Coronagraph (LASCO). *Solar Phys.* **1995**, *162*, 357–402.
61. SOHO / Solar and Heliospheric Observatory. Available online: http://sohowww.nascom.nasa.gov/ (Accessed on 6 May 2010).
62. Chen, J.; Howard, R.A.; Brueckner, G.E.; Santoro, R.; Paswaters, S.E., St. Cyr, O.C.; Schwenn, R.; Lamy, P.; Simnett, G.M. Evidence of an erupting magnetic flux rope: LASCO coronal mass ejection of 1997 April 13. *Astrophys. J.* **1997**, *490*, L191–L194.
63. Wood, B.E.; Karovska, M.; Chen, J.; Brueckner, G.E.; Cook J.W.; Howard, R.A. Comparison of two coronal mass ejections observed by EIT and LASCO with a model of an erupting magnetic flux rope. *Astrophys. J.* **1999,** *512*, 484–495.
64. Krall, J.; Chen, J.; Duffin, R.T.; Howard, R.A.; Thompson, B.J. Erupting solar magnetic flux ropes: Theory and observation. *Astrophys. J.* ***2001***, *562*, 1045–1057.
65. Shafranov, V.D. Plasma equilibrium in a magnetic field. In *Reviews of Plasma Physics*; Leontovich, M.A., Ed.; Consult. Bureau: New York, NY, USA; pp. 103–151.
66. Chen, J.; Marque, C.; Vourlidas, A.; Krall, J.; Schuck, P.W. The flux-rope scaling of the acceleration of coronal mass ejections and eruptive prominences. *Astrophys. J.* **2006**, *649*, 452–463.
67. Chen, J. Comment on "Torus Instability". *Phys. Rev. Lett.* **2007**, *99*, 099501.
68. Devore, C.R.; MacNeice, P.J.; Olson, K.M. An adaptively refined MHD solver for solar, space and astrophysical simulations. *Bull. Am. Phys. Soc. DCOMP Meeting 2001 Scientific Program,* **2001**, *46*, *Part F*, R1.001.
69. Boris, J.P.; Book, D.L. Flux-corrected transport: I: SHASTA, a fluid transport algorithm that works. *J. Comput. Phys.* **1973**, *11*, 1–38.
70. Linton, M.G.; Devore, C.R.; Longcope, D.W. Patchy Reconnection in a Y-Type Current Sheet. *Earth Planets Space* **2008**, *61*, 573–576.
71. Yamada, M.; Ji, H.; Hsu, S.; Carter, T.; Kulsrud, R.; Bretz, N.; Jobes, F.; Ono, Y.; Perkins, F. Study of driven magnetic reconnection in a laboratory plasma. *Phys. Plasmas* **1997**, *4*, 1936–1944.

72. Linton, M.G.; Dahlburg, R.B.; Antiochos, S.K. Reconnection of twisted flux tubes as a function of contact angle. *Astrophys. J.* **2001**, *553*, 905–921.
73. Dahlburg, R.B.; Horton, W.; Rowan, W.L.; Correa, C.; Perez, J.C. Evolution of the bounded magnetized jet and comparison with Helimak experiments. *Phys. Plasmas* **2009**, *16*, Art. No. 072109.
74. Dahlburg, R.B.; Antiochos, S.K.; Zang, T.A. Secondary instability in three-dimensional magnetic reconnection. *Phys. Fluids B* **1992**, *4*, 3902–3914.
75. Dahlburg, R.B.; Klimchuk, J.A.; Antiochos, S.K. An explanation for the 'switch on' nature of magnetic energy release and its application to coronal heating. *Astrophys. J.* **2005**, *622*, 1191–1201.